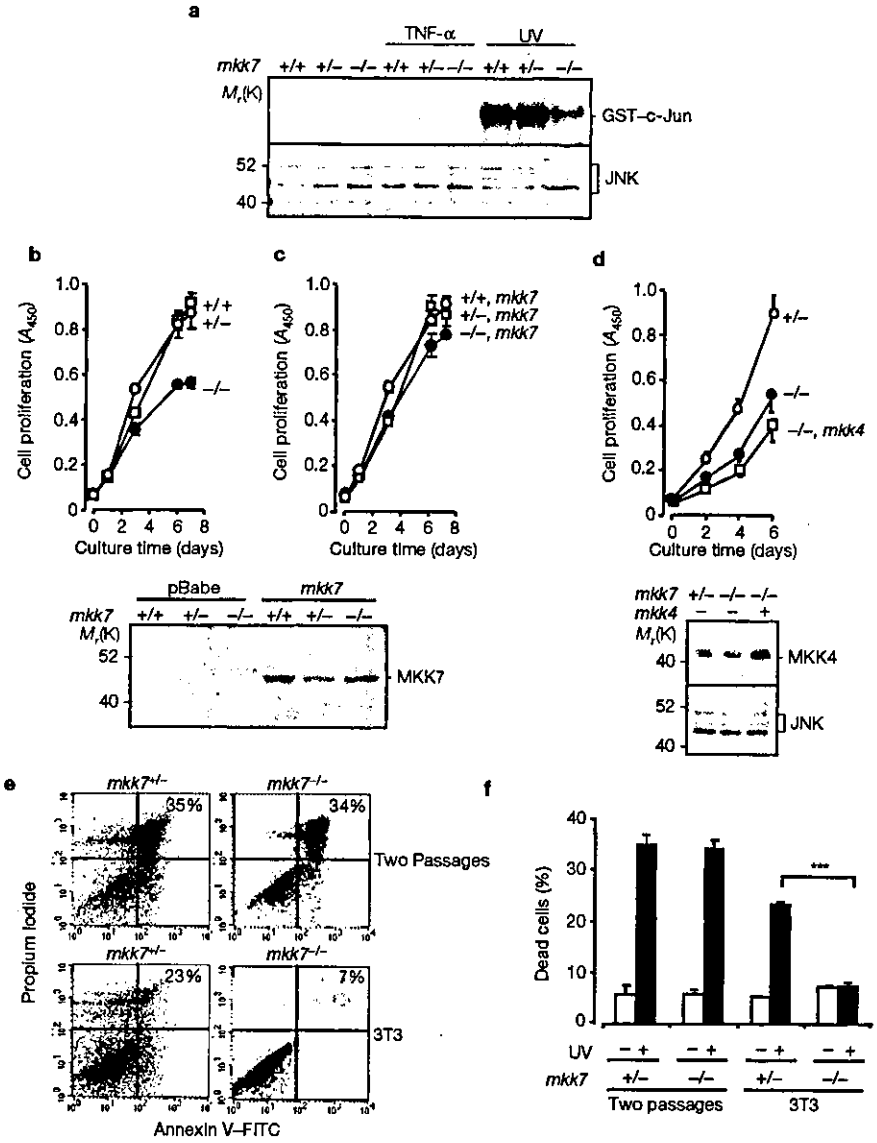

Figure 2 Decreased proliferation and premature senescence of *mkk7*$^{-/-}$ MEFs. (**a**) JNK activity in serum-starved (0.5% serum for 3 days) *mkk7*$^{+/+}$, *mkk7*$^{+/-}$ and *mkk7*$^{-/-}$ MEFs (passage 3) stimulated with TNF-α (10 ng ml^{-1}) and UV (10 J m^{-2}). JNK activity was determined by immune-complex kinase assay using GST–c-Jun as a substrate. (**b–d**) Decreased proliferation of *mkk7*$^{-/-}$ MEFs (passage 4; **b**), and reversal of the proliferation defect by ectopic expression of wild-type MKK7 (**c**), but not by over-expression of wild-type MKK4 (**d**). pBabe (control, **b**), pBabe-MKK7 (**c**) and pBabe-MKK4 (**d**) were introduced into MEFs, and proliferation was determined at the indicated times. Western blots show expression levels of each protein after infection (for the whole blots of **a**, **c** and **d**, see Supplementary information, Fig. S2c–e). In **b**, $P < 0.01$ between *mkk7*$^{+/+}$ or *mkk7*$^{+/-}$ and *mkk7*$^{-/-}$ MEFs (Students *t*-test). (**e**, **f**) Apoptosis in *mkk7*$^{+/-}$ and *mkk7*$^{-/-}$ MEFs. Passage-2 MEFs and 3T3 MEFs were left untreated or were irradiated with 10 J m^{-2} UV 24 h before determination of cell death by annexinV/PI staining. Quantification of three different assays (**f**) and typical annexinV/PI FACS profiles of UV-irradiated MEFs (**e**) are shown. ***$P < 0.001$ between UV-treated *mkk7*$^{+/-}$ and *mkk7*$^{-/-}$ MEFs (Student's *t*-test). In all figures, error bars are shown as standard error of the mean (s.e.m.).

ies[15], loss of MKK7 expression resulted in impaired JNK activation in MEFs at the basal level and after stimulation with tumour necrosis factor α (TNF-α) or UV irradiation (Fig. 2a). Activation and expression of p38-MAPK in MEFs were unaffected in *mkk7*$^{-/-}$ MEFs (data not shown). During the first three passages, cell proliferation was comparable between *mkk7*$^{+/+}$, *mkk7*$^{+/-}$ and *mkk7*$^{-/-}$ MEFs (data not shown). From passages 4–5 onwards, all *mkk7*$^{-/-}$ MEFs analysed showed significantly reduced proliferation under baseline culture conditions (Fig. 2b) and after serum stimulation (data not shown). In all experiments, *mkk7*$^{+/-}$ MEFs behaved similarly to *mkk7*$^{+/+}$ MEFs. Re-expression of wild-type MKK7 (Fig. 2c) restored the reduced proliferation of *mkk7*$^{-/-}$ MEFs to levels observed in wild-type MEFs. Consistent with recent data showing that both MKK4 and MKK7 are required to synergistically activate JNKs[8–10], overexpression of the second JNK activating kinase, MKK4, could not substitute for the loss of MKK7 (Fig. 2d).

To test whether the reduced proliferation in *mkk7*$^{-/-}$ MEFs was

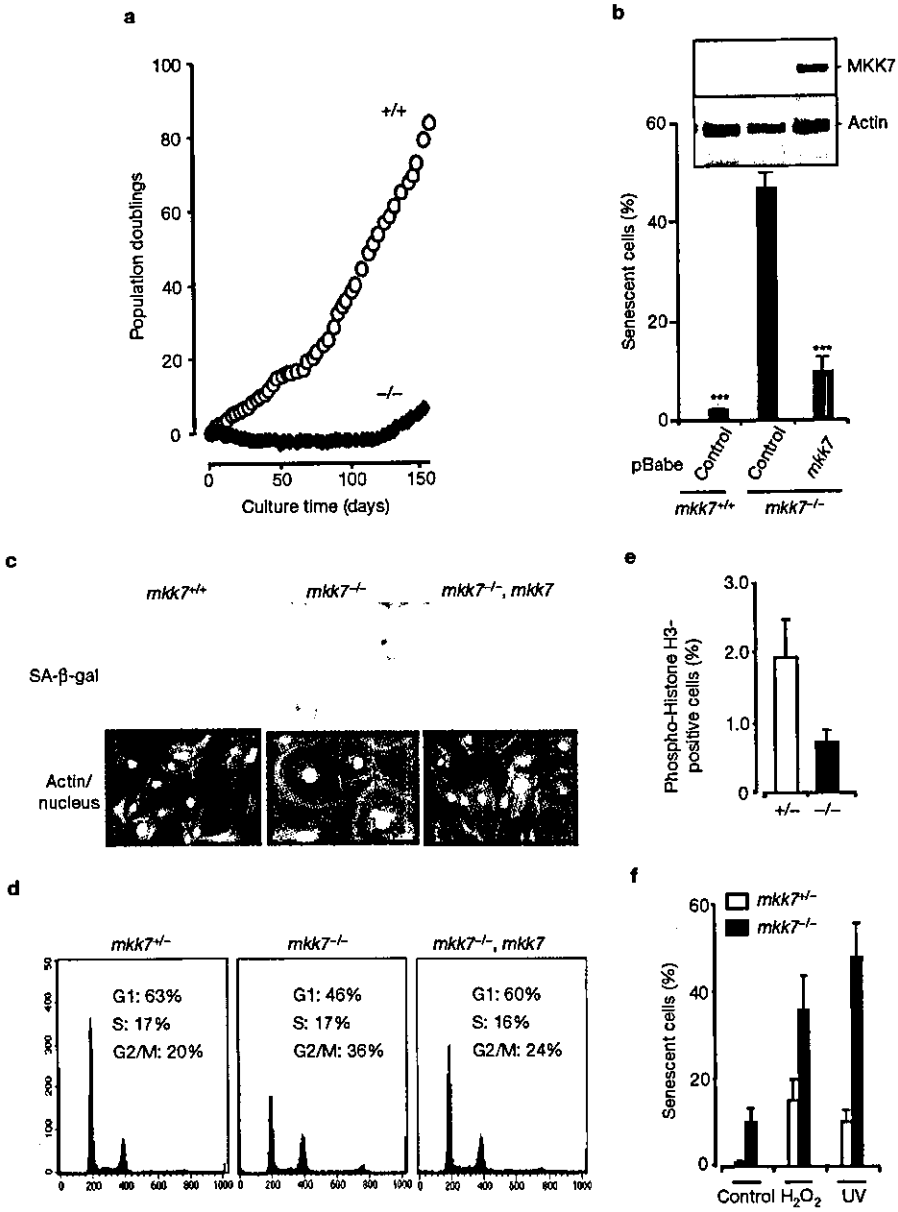

Figure 3 MKK7 is required to protect cells from premature senescence. **(a)** Typical growth curves of *mkk7*$^{+/+}$ and *mkk7*$^{-/-}$ MEFs. One representative experiment out of five is shown. **(b)** Senescence in *mkk7*$^{+/+}$ and *mkk7*$^{-/-}$ MEFs infected with empty pBabe vector (controls) or wild-type MKK7. Senescence was determined at passage 5 by SA-β-galactosidase staining. Western blots show expression levels of each protein after infection (for whole blots, see Supplementary Information, Fig. S2f). ***$P < 0.001$ versus *mkk7*$^{-/-}$ MEFs infected with control pBabe. **(c)** Microscopic analysis of *mkk7*$^{+/+}$, *mkk7*$^{-/-}$ and *mkk7*$^{-/-}$ MEFs expressing wild-type MKK7. SA-β-galactosidase staining (SA-β-gal) is shown in top panels. In the bottom panels, phalloidin–rhodamine (red) was used to stain actin and DAPI (blue) was used to stain nuclei. Representative data from passage-5 cells are shown. Note the flattened and rounded shapes of *mkk7*$^{-/-}$ fibroblasts characteristic of senescent cells. **(d)** Increased G2/M boundaries in *mkk7*$^{-/-}$ MEFs (passage 5) that can be rescued by ectopic expression of wild-type MKK7, but not kinase-dead MKK7 (data not shown). Typical PI FACS analysis is shown for passage-5 MEFs. Some of the *mkk7*$^{-/-}$ cells seem to have greater than 4N DNA content, although this is not a consistent result. **(e)** Numbers of phosphorylated Histone H3-positive cells in *mkk*$^{+/-}$ and *mkk7*$^{-/-}$ MEFs (passage 5) using phospho-specific anti-Histone H3 (Ser10) antibodies. Mean values from three independent experiments are shown. **(f)** *mkk7*$^{+/-}$ and *mkk7*$^{-/-}$ MEFs (passage 3) were UV-irradiated (10 J m^{-2}) or treated with H_2O_2 (150 μM). Stress-induced senescence (mean numbers of SA-β-galactosidase-positive cells) was determined 3 days after stress. The senescent phenotype was confirmed by examination of cell morphology. In addition, increased numbers of cells at the G2/M boundary were observed in those cells (data not shown).

caused by cell-cycle arrest and/or enhanced apoptosis, we first analysed the susceptibility of *mkk7*$^{-/-}$ and *mkk7*$^{+/-}$ MEFs to death stimuli. In particular, it has been shown previously that inactivation of the JNK pathway in MEFs results in resistance to UV-induced cell death[16,17]. Early passage *mkk7*$^{+/-}$ and *mkk7*$^{-/-}$ MEFs showed comparable levels and kinetics of cell death in response to UV- or γ-irradiation (Fig. 2e, f

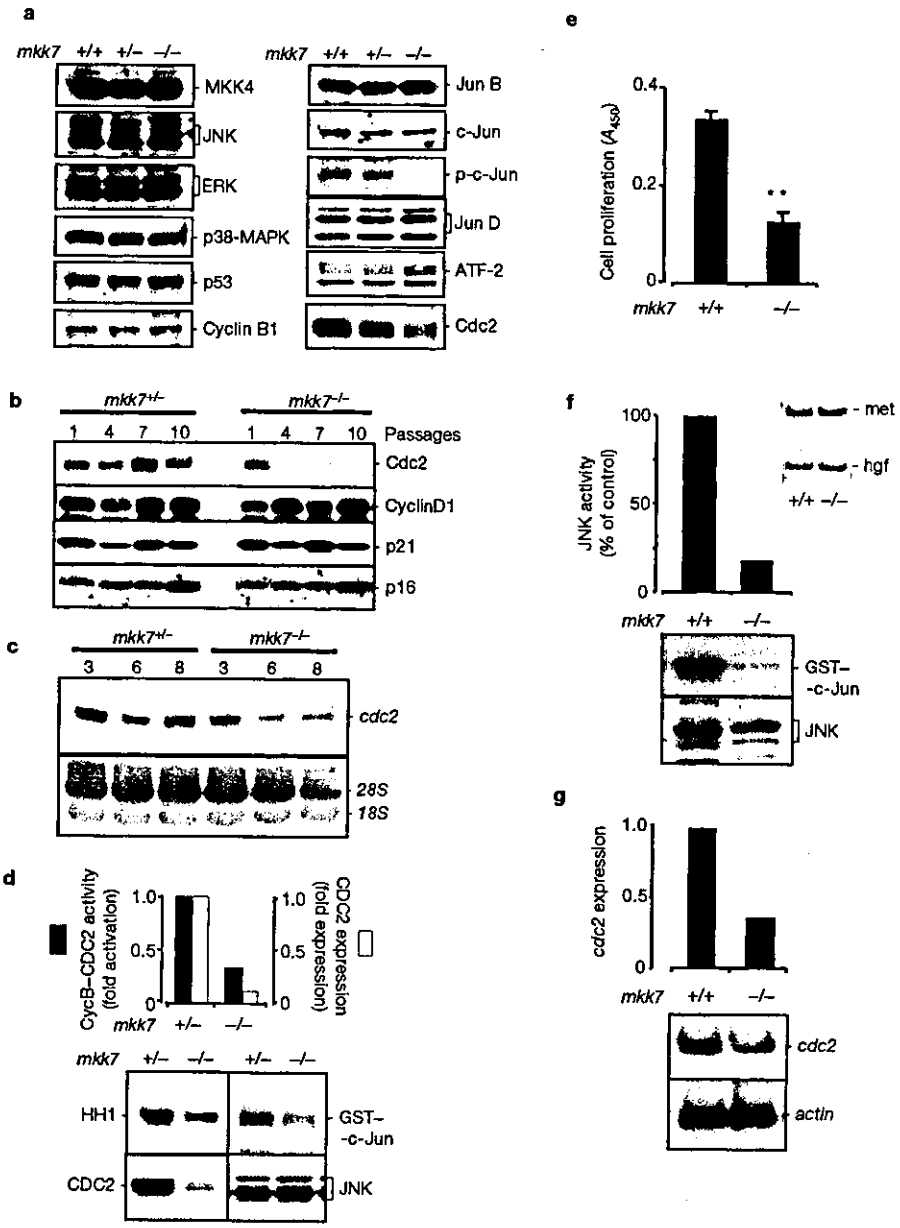

Figure 4 Loss of MKK7 results in decreased CDC2 expression and reduced CDC2 kinase activity. **(a)** Expression levels of the indicated signalling and cell cycle molecules were determined by western blotting of passage-4 *mkk7*$^{+/+}$, *mkk7*$^{+/-}$ and *mkk7*$^{-/-}$ MEFs under normal culture conditions. **(b)** Expression levels of CDC2, cyclinD1, p16 and p21 in passage-1, -4, -7 and -10 *mkk7*$^{+/-}$ and *mkk7*$^{-/-}$ MEFs. **(c)** Reduced expression level of *cdc2* mRNA in *mkk7*$^{-/-}$ MEFs (passage 3, 6 and 8). Total RNA, stained with methylene blue, is shown in the lower panel. **(d)** Decreased cyclin B1–CDC2 complex kinase activity in *mkk7*$^{-/-}$ MEFs (passage 5). CDC2 kinase and JNK activities were determined using Histone H1 (HH1) and GST–c-Jun as substrates. **(e)** Proliferation of embryonic hepatocytes (3×10^3 cells per well) isolated from E11.5 *mkk7*$^{+/-}$ and *mkk7*$^{-/-}$ littermate embryos. $^{**}P < 0.01$. **(f)** Impaired JNK activation in hepatocytes purified from E11.5 *mkk7*$^{-/-}$ embryos. Hepatocytes were stimulated with HGF (30 ng ml^{-1}) for 15 min and then JNK activity was determined by immune-complex kinase assays. Insets show normal levels of *c-Met* and *HGF* mRNA expression in *mkk7*$^{-/-}$ liver cells. **(g)** Decreased expression of *cdc2* mRNA in hepatocytes from E11.5 *mkk7*$^{-/-}$ embryos. Embryonic hepatocytes were isolated as in **e** and quantitative RT–PCR was performed with α-^{32}P-dCTP. PCR products were detected with a phosphoimager. For the whole blots of **a**–**d**, **f** and **g**, see Supplementary Information, Figs S3a–d and 4a, b.

and not shown). Moreover, spontaneous cell death was comparable between the two genotypes at early passages. However, at later times of culture, *mkk7*$^{-/-}$ 3T3 cells showed resistance to UV-irradiation induced cell death (Fig. 2e, f). Our results indicate that the 'history' and passage number of cells is a critical determinant for cell death susceptibility in the absence of MKK7 expression. Importantly, our data show that

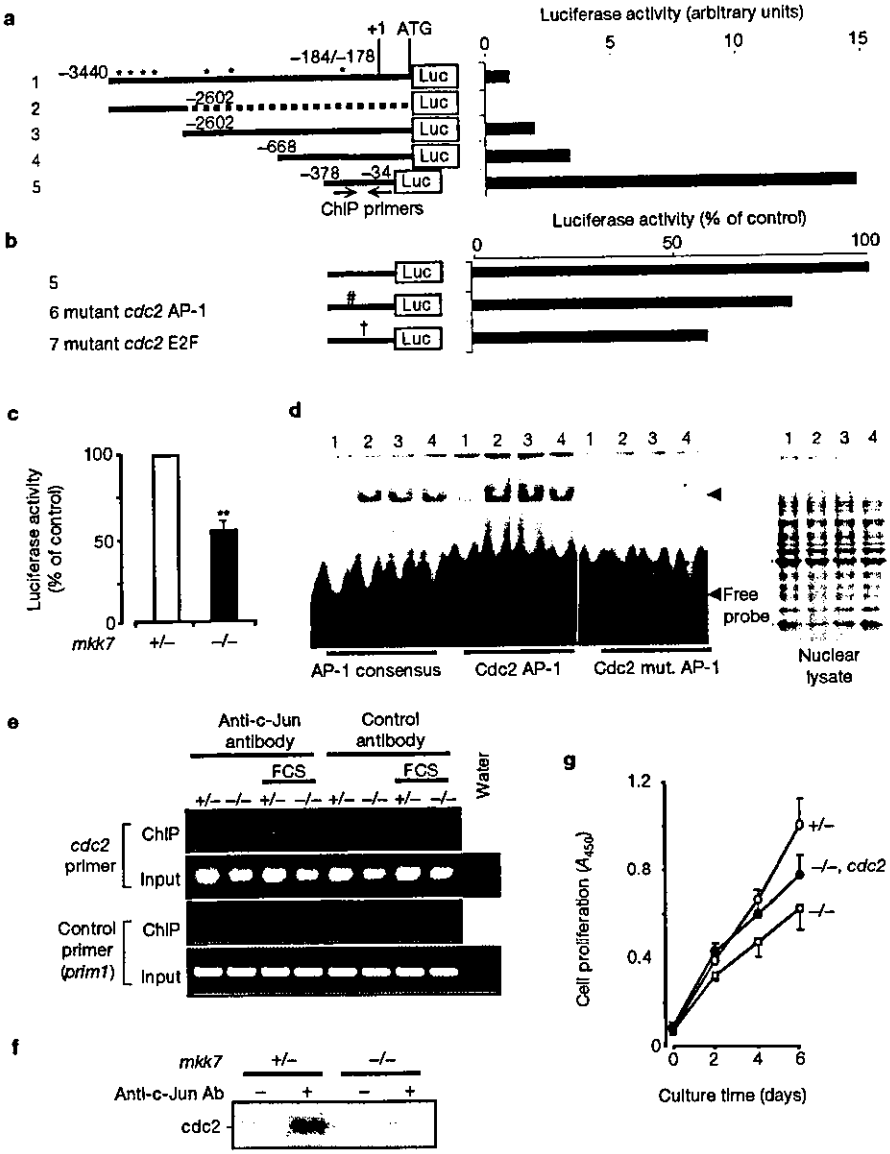

Figure 5 MKK7 controls *cdc2* promoter activity. (**a**, **b**) MKK7 enhances *cdc2* promoter activity in luciferase reporter assays. The indicated constructs were transfected into phoenix E cells and luciferase activities were measured. Potential AP-1-binding sites based on *in silico* analysis are indicated with an asterisk. E2F and *cdc2* AP-1 mutations are indicated as # and †, respectively. Mean values of three experiments are shown. (**c**) Luciferase reporter assays in *mkk7*$^{+/-}$ and *mkk7*$^{-/-}$ MEFs (passage 4). Construct 5 in **a** was used to determine *cdc2* promoter activity. One representative experiment is shown. $^{**}P < 0.01$ between *mkk7*$^{+/-}$ and *mkk7*$^{-/-}$ MEFs. (**d**) Cell extracts were obtained from wild-type MEFs, and EMSAs were performed using consensus AP-1, wild-type *cdc2* AP-1, and mutant *cdc2* AP-1 oligonucleotides. Lane 1, 0.5% serum-starved cells; lane 2, exponentially proliferating cells; lane 3, 20% serum stimulation (30 min); lane 4, 10 J m^{-2} UV stimulation. The right panel shows the amounts of nuclear lysates as loading controls. (**e**, **f**) ChIP assay of c-Jun bound to the *cdc2* AP-1 site in *mkk7*$^{+/-}$and *mkk7*$^{-/-}$ MEFs (passage 4). The positions of the ChIP primers are shown in **a**. The primers for *prim1* gene, which is located on the same chromosome as *cdc2* and does not contain AP-1 consensus sequences in its promoter locus, were used as control. Input indicates total cell lysates before immunoprecipitation to ensure equal loading. ChIP PCR products were visualized using ethidium bromide staining (**e**) or α-^{32}P-dCTP incorporation (**f**). (**g**) Ectopic expression of wild-type CDC2 partially restores the decreased proliferation of passage-4 *mkk7*$^{-/-}$ MEFs. Mean proliferation values of three experiments are shown.

reduced proliferation of *mkk7*$^{-/-}$ MEFs is not the result of increased cell death.

To determine the role of MKK7 in cell proliferation, MEFs were cultured for over 150 days. Similarly to our proliferation data, *mkk7*$^{-/-}$ MEFs did not show any significant differences in population doubling within the first three passages (Fig. 3a). However, during subsequent passages, loss of MKK7 resulted in a marked decrease in cell numbers (Fig. 3a). In all MEF cell lines (five independent cultures) analysed, loss

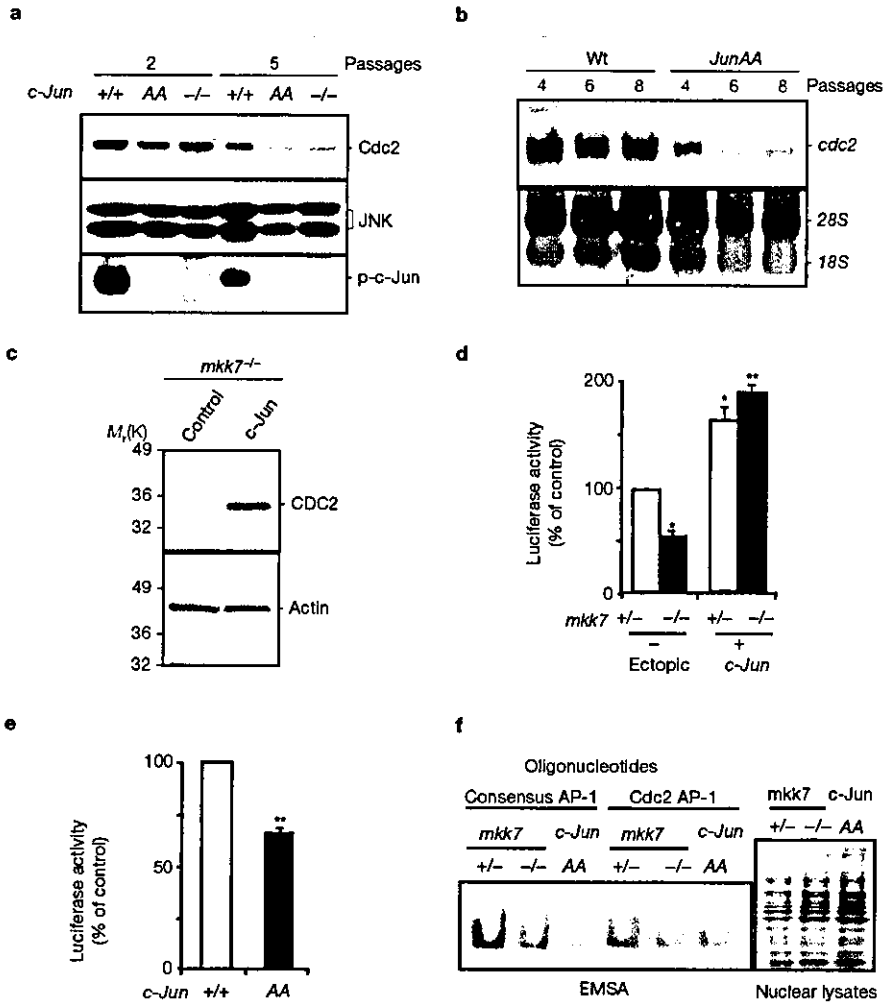

Figure 6 c-Jun regulates CDC2 expression. (**a**) Expression levels of CDC2 protein, JNK and phospho-c-Jun in passage-2 and -5 *c-jun*$^{-/-}$ and *c-junAA* MEFs. (**b**) Expression levels of *cdc2* mRNA in passage-4, -6 and -8 wild-type and *c-junAA* MEFs. Total RNA, stained with methylene blue, is also shown (bottom). (**c**) Overexpression of c-Jun upregulates CDC2. pBabe (control) or pBabe-c-Jun were introduced into *mkk7*$^{-/-}$ MEFs and CDC2 protein expression was determined by western blotting. For the whole blots of **a**–**c**, see Supplementary Information Fig. S4c–e. (**d**) Luciferase reporter assays in *mkk7*$^{+/-}$ *and mkk7*$^{-/-}$ MEFs in the presence and absence of overexpressed c-Jun (passage 4). pBabe-c-Jun or pBabe were introduced in MEFs and construct 5 from Fig. 5a was used to determine *cdc2* promoter activity. $^{*}P < 0.05$. $^{**}P < 0.01$ versus *mkk7*$^{+/-}$ MEFs transfected with control pBabe. (**e**) Luciferase reporter assays of *cdc2* promoter activity in c-*junAA* MEFs. $^{**}P < 0.01$ between *c-JunAA* and wild-type control MEFs. (**f**) EMSA assay in *mkk7*$^{+/-}$, *mkk7*$^{-/-}$ and *c-JunAA* MEF cell extracts using consensus AP-1 and *cdc2* AP-1. The right panel shows loading of nuclear lysates.

of MKK7 resulted in extended crisis and premature senescence, as determined by senescence-associated β-galactosidase (SA-β-gal) staining (Fig. 3b and top panel in Fig. 3c) and an enlarged and flattened cell morphology (Fig. 3c, bottom), both of which are established features of senescence in MEFs[18]. Ectopic expression of wild-type MKK7, but not kinase-dead MKK7, rescued premature senescence in *mkk7*$^{-/-}$ MEFs (Fig. 3b, c, and data not shown). Overexpression of MKK7 also increased proliferation and delayed the onset of crisis and senescence in wild-type MEFs (data not shown). Moreover, genetic inactivation of MKK4 in MEFs resulted in reduced proliferation doubling times and premature senescence, indicating that both MKK4 and MKK7 are essential for these cellular processes (data not shown). These results are consistent with previous data showing that loss of JNK1/JNK2 in MEFs results in reduced proliferation[17] and that inactivation of c-Jun in MEFs results in premature senescence and impaired proliferation[19]. Thus, the MKK4–MKK7-regulated JNK signalling pathway is directly responsible for the control of proliferation and cellular senescence.

Defective G2/M cell-cycle progression

As *mkk7*$^{-/-}$ MEFs undergo premature senescence and display reduced proliferation, we analysed the cell-cycle profiles in *mkk7*$^{-/-}$ MEFs after five passages. Surprisingly, whereas senescent cells are normally arrested at the G1 phase[20], *mkk7*$^{-/-}$ MEF lines displayed more G2/M

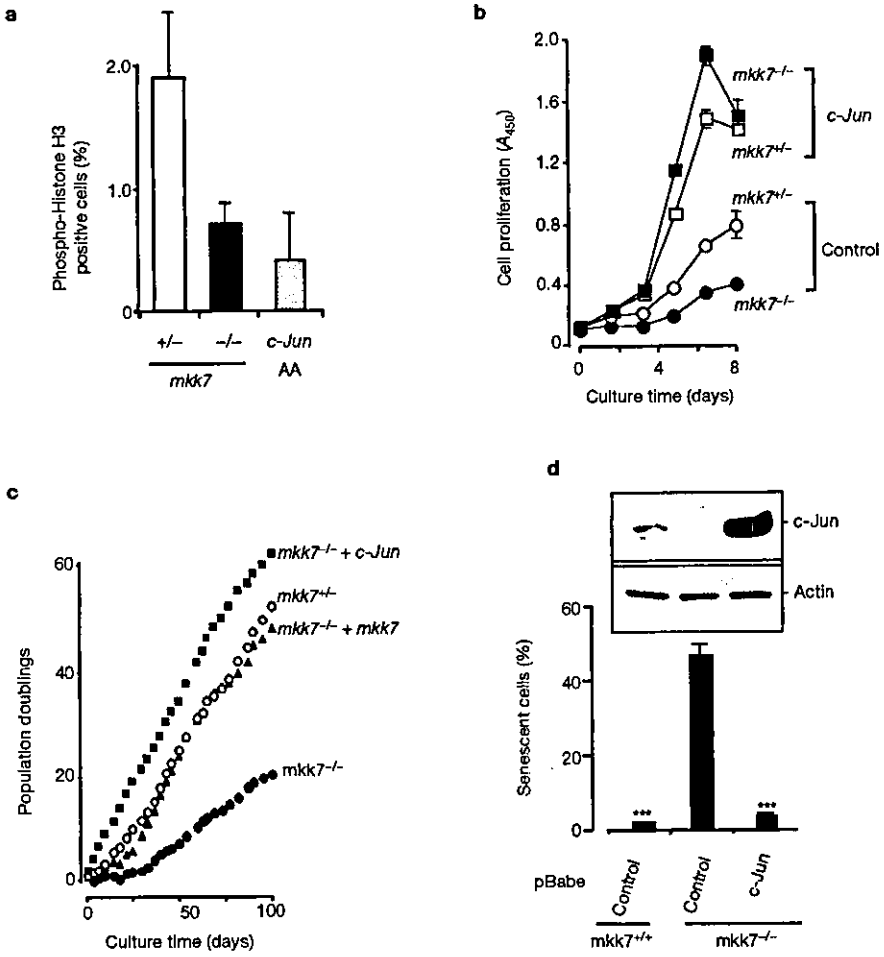

Figure 7 c-Jun rescues senescence and proliferation defects in *mkk7*$^{-/-}$ MEFs. (a) Phospho-Histone H3-positive cells in *mkk7*$^{+/-}$, *mkk7*$^{-/-}$ and *c-JunAA* MEFs. Mean values from three independent experiments are shown. (b) Cell proliferation (passage 4) was determined at the indicated times. pBabe (control) or pBabe-c-Jun was introduced into *mkk7*$^{+/-}$ and *mkk7*$^{-/-}$ MEFs. (c) Growth curves of *mkk7*$^{+/-}$ and *mkk7*$^{-/-}$ MEFs. pBabe (control), pBabe-c-Jun or pBabe-MKK7 were introduced into *mkk7*$^{+/-}$ and *mkk7*$^{-/-}$ MEFs and population doublings were determined as in Fig. 3a. (d) c-Jun overexpression rescues cellular senescence of *mkk7*$^{-/-}$ MEFs. Senescence was determined at passage 5 by SA-β-galactosidase staining. Western blots show expression levels of c-Jun and β-actin (for whole blots, see Supplementary Information Fig. S4f). ***$P < 0.001$ versus *mkk7*$^{-/-}$ MEFs.

boundaries when compared with *mkk7*$^{+/-}$ (Fig. 3d) or wild-type (data not shown) MEFs. Re-expression of MKK7 in *mkk7*$^{-/-}$ MEFs abolished the G2/M cell-cycle arrest (Fig. 3d). Synchronized *mkk7*$^{-/-}$ MEFs did not show an apparent defect in G1-to-S-phase entry; however, *mkk7*$^{-/-}$ MEFs displayed an extended G2/M phase after serum stimulation (data not shown). To address whether *mkk7*-deficient MEFs are arrested in G2 or M phase, phospho-Histone H3 staining was performed. Histone H3 is phosphorylated at Ser 10 during M phase, but not at G2 (refs 21, 22). *mkk7*$^{-/-}$ MEFs showed less phospho-Histone H3-positive cells than *mkk7*$^{+/-}$ cells (Fig. 3e), indicating that *mkk7*$^{-/-}$ MEFs are arrested in G2 phase rather than M phase. These data show that loss of MKK7 in MEFs results in an unexpected defect in G2/M cell-cycle progression.

Interestingly, environmental stresses, such as UV irradiation and oxidative stress, trigger a G2/M arrest[23–25] and premature senescence[26]. Therefore, low-passage *mkk7*$^{+/-}$ and *mkk7*$^{-/-}$ MEFs were treated with hydrogen peroxide and UV to test the role of the MKK7–JNK in G2/M arrest and senescence in response to these environmental stresses. *mkk7*$^{-/-}$ MEFs displayed more susceptibility to stress-induced premature senescence (Fig. 3f) and G2/M block (see Supplementary Information, Fig. S2a, b). Thus, MKK7 regulates cellular senescence and G2/M progression in response to environmental stress

Impaired CDC2 expression and CDC2 activity in *mkk7*$^{-/-}$ MEFs

To identify the mechanism through which MKK7 regulates proliferation and G2/M cell cycle progression, we examined the expression levels of molecules known to be involved in cell-cycle control and senescence. Expression of ERK1/2, p38-MAPK, MKK4, JNKs, JunB, JunD, and ATF2 were comparable between *mkk7*$^{+/+}$, *mkk7*$^{+/-}$, and *mkk7*$^{-/-}$ MEFs (Fig. 4a). Consistent with the *in vitro* kinase assays showing reduced JNK activation (Fig 2a), phosphorylation and expression of c-Jun were reduced in *mkk7*$^{-/-}$ MEFs (Fig. 4a). Expression of the cell-cycle molecules cyclin B (Fig. 4a), p16, p21, cyclin D1 (Fig. 4b), p27 and cyclin E (data not shown) were comparable between the different genotypes. Similarly to previously results[15], we did not observe obvious changes in

p53 expression (Fig. 4a). Moreover, telomerase activity in *mkk7*$^{-/-}$ MEFs was comparable with MKK7-expressing MEFs (data not shown).

Intriguingly, a marked reduction in the expression of CDC2 protein was observed (Fig. 4a). CDC2 has been shown to be essential for G2/M cell-cycle progression in multiple organisms[27,28]. Reduced expression of CDC2 in *mkk7*$^{-/-}$ MEFs correlated with the numbers of cell passages; CDC2 expression seemed normal at early passages (passage 1–2: normal G2/M phase, proliferation and population doubling), and consistent with the proliferation defect, it was rapidly downregulated thereafter (passage 4–10: G2/M block and reduced proliferation and population doubling; Fig. 4b). Expression levels of cyclin D1, p21, p16 (Fig. 4b), p53, GADD45 and JNK (data not shown) were similar in *mkk7*$^{+/-}$ and *mkk7*$^{-/-}$ MEFs at the different passage numbers examined. *mkk7*$^{-/-}$ MEFs exhibited reduced JNK activation and delayed CDC2 up-regulation after serum stimulation (data not shown). Reduced expression of *cdc2* mRNA was also observed in *mkk7*$^{-/-}$ MEFs (Fig. 4c). Importantly, cyclin B1-associated CDC2 kinase activity was markedly reduced in *mkk7*$^{-/-}$ MEFs (Fig. 4d), indicating that reduced CDC2 expression correlates with impaired cyclin B1/CDC2 activity. These data suggest that CDC2 is a potential molecular target for MKK7 regulated stress kinase signalling.

Impaired proliferation and CDC2 expression in primary *mkk7*$^{-/-}$ hepatocytes

Whereas hepatogenesis seemed normal at earlier stages of embryogenesis in *mkk7*$^{-/-}$ embryos, mutation of MKK7 results in embryonic lethality that correlated with impaired liver development (Fig. 1). The defective development of the parenchymal liver in *mkk7*$^{-/-}$ embryos seemed to parallel our results in *mkk7*-null MEFs, which display normal proliferation at initial passages that is rapidly followed by a proliferation defect. Therefore, proliferation was analysed in hepatocytes and haematopoietic liver progenitor cells from E11.5 *mkk7*$^{-/-}$ embryos. Haematopoietic precursor cells from both *mkk7*$^{+/-}$ and *mkk7*$^{-/-}$ embryos stained positive for 5-bromo-2'-deoxyuridine (BrdU) labelling *in vivo*, indicating that these cells were proliferating (data not shown). In addition, using *in vitro* clonal differentiation assays[11], *mkk7*$^{-/-}$ and *mkk7*$^{+/-}$ precursors derived from the liver of E10.5 embryos developed into macrophages/monocytes, mast cells and immunoglobulin-secreting B lymphocytes (data not shown). Thus, haematopoietic precursors present in *mkk7*$^{-/-}$ liver remnants can give rise to various haematopoietic cell lineages. In contrast, proliferation of hepatocytes was markedly impaired in E11.5 *mkk7*$^{-/-}$ embryos, as determined by BrdU *in vivo* labelling (data not shown). Reduced proliferation of hepatocytes was also observed in primary hepatocyte cultures isolated from *mkk7*$^{-/-}$ E11.5 embryos (Fig. 4e). JNK activation was abolished in these primary *mkk7*$^{-/-}$ hepatocytes in response to hepatocyte growth factor (HGF) treatment (Fig. 4f). Similarly to *mkk7*$^{-/-}$ MEFs, *cdc2* mRNA expression was downregulated in primary *mkk7*$^{-/-}$ hepatocytes (Fig. 4g). Thus, these results suggest that the MKK7–JNK signalling pathway is important for CDC2 expression, and proliferation of MEFs and primary hepatocytes.

CDC2 is a target for MKK7–JNK signalling

Reduced CDC2 expression in *mkk7*$^{-/-}$ MEFs could be an indirect consequence of premature senescence, or CDC2 could be a direct target of the MKK7–JNK signalling pathway. MKK7 or JNK was not co-immunopreciptated with CDC2/ cyclin B1 and phosphorylation of CDC2/ cyclin B1 by recombinant MKK7 or recombinant JNK was not observed using *in vitro* kinase assays (data not shown). *In silico* analysis of the murine *cdc2* promoter region identified several predicted AP-1 elements in the −3,440 to +1 bp region (Fig. 5a, asterisks). Luciferase promoter assays using deletion mutants in phoenixE cells showed that the sequence 5'-AGAGTCA-3' at −184/−178 of the *cdc2* promoter is a potential AP-1 site required for effective *cdc2* transactivation (Fig. 5a). It should be noted that the identical promoter sequence has been previously identified in the prostaglandin G/H synthase-2 promoter[29]. Treatment with TPA (12-O-tetradecanoylphorbol-13-acetate) and serum induce binding to oligonucleotides containing the 5'-AGAGTCA-3' sequence, and antibodies specific for c-Jun and c-Fos inhibit binding of AP-1 to the prostaglandin G/H synthase-2 promoter in electromobility shift assays (EMSAs) [29]. Mutation of the *cdc2* AP-1 site rendered lower promoter transactivation in our luciferase assays, albeit to a lesser extent than a mutation in the previously defined[30] *cdc2* promoter −129/−121 E2F-binding site (Fig. 5b). Whether additional AP-1 sites are critical in the CDC2 promoter remains to be determined. Furthermore, transactivation of a *cdc2*-promoter–luciferase reporter construct was impaired in *mkk7*$^{-/-}$ MEFs (Fig. 5c).

In EMSA assays (Fig. 5d), both the consensus AP-1 site and the 5'-AGAGTCA-3' AP-1 site present in the cdc2 promoter showed band shifts after incubation in serum and UV stimulation. Mutation of the −184/−178 *cdc2* AP-1 site abolished the band shift (Fig. 5d). To determine whether c-Jun, the downstream target of MKK7–JNK, can bind to the *cdc2* promoter region under physiological conditions, chromatin immunoprecipitation (ChIP) analysis was performed (Fig. 5e). The *cdc2* promoter region encompassing the −184/−178 AP-1 site was precipitated in the presence of an anti-c-Jun specific antibody, indicating that c-Jun can bind to the *cdc2* promoter but does not bind to the control *prim1* gene promoter region present on the same chromosome (Fig. 5e). Binding of c-Jun to the *cdc2* promoter in ChIP experiments was confirmed by radioactive PCR (Fig. 5f). To test whether CDC2 is important for cell proliferation in *mkk7*$^{-/-}$ MEFs, wild-type CDC2 was over-expressed. Ectopic expression of wild-type CDC2 in *mkk7*$^{-/-}$ MEFs partially restored proliferation (Fig. 5g). These data identify CDC2 as a target of the MKK7–JNK signalling pathway and indicate that CDC2 might be important for overcoming the cell cycle block of *mkk7*-null cells. However, we cannot rule out the possibility that CDC2 expression might also be controlled indirectly by other MKK7–JNK–c-Jun-regulated molecules, as the direct effect of c-Jun on *cdc2* promoter activity is not strong.

Control of CDC2 expression, senescence and G2/M progression by c-Jun

The MKK7–JNK stress pathway regulates gene transcription through phosphorylation of multiple transcription factors, including c-Jun or ELK-1 (refs 1–5). As we observed reduced phosphorylation and expression of c-Jun in *mkk7*$^{-/-}$ fibroblasts (Fig. 4a), and c-Jun controls the *cdc2* promoter (Fig. 5), we wanted to confirm the role of c-Jun in cellular senescence, G2/M progression and CDC2 expression in genetic experiments.

Consistent with the impaired phosphorylation of c-Jun and reduced CDC2 expression in *mkk7*$^{-/-}$ MEFs, *c-jun*$^{-/-}$ MEFs also displayed reduced expression of CDC2 protein at later passages (Fig. 6a). Importantly, MEFs derived from *c-junAA* mutant mice carrying a mutant of both c-Jun phosphorylation sites[13,14] also showed reduced CDC2 protein (Fig. 6a), as well as reduced *cdc2* mRNA expression after more than five passages (Fig. 6b). Over-expression of c-Jun in *mkk7*$^{-/-}$ MEFs restored CDC2 expression (Fig. 6c) and transactivation of the *cdc2* AP-1 promoter construct to levels observed in wild-type MEFs (Fig. 6d). Activity of the *cdc2* promoter construct was also reduced in *c-junAA* MEFs (Fig. 6e). Moreover, in EMSA experiments binding of MEF extracts to consensus AP-1 and *cdc2* AP-1 oligonucleotides were reduced in both *mkk7*$^{-/-}$ and *c-junAA* MEFs (Fig. 6f). These data show

that CDC2 expression can be regulated by the MKK7–JNK–c-Jun signalling pathway.

To evaluate whether c-Jun controls G2/M progression, cell-cycle analysis was performed in early passage *c-jun*$^{-/-}$ and *c-junAA* MEFs. Similarly to *mkk7*$^{-/-}$ MEFs, loss of c-Jun or inactivation of the JNK phosphorylation sites of c-Jun resulted in the accumulation of cells at the G2/M boundaries beginning from passage 4 (Table 2). Immunostaining with phospho-Histone H3 confirmed that the arrest occurred at the G2 phase, rather than the M phase (Fig. 7a). Importantly, over-expression of c-Jun rescued the defects in proliferation and premature senescence observed in *mkk7*$^{-/-}$ MEFs (Fig. 7b–d). These data suggest an involvement of the MKK7–JNK–c-Jun pathway in G2/M cell cycle progression and cell proliferation in MEFs.

DISCUSSION

Our results show that MKK7 and c-Jun are critical for MEF proliferation and G2/M cell-cycle progression. Previous data from other groups have shown that the JNK–c-Jun signalling pathway is required to promote proliferation in primary MEFs[17,19,32]. However, it has been shown recently that JNK1/JNK2 signalling may attenuate proliferation after Ras-mediated transformation in 3T3 cells[32]. It should be noted that overexpression of Ras causes premature cellular senescence in primary MEFs, whereas it can transform most immortalized cells (such as 3T3 MEFs) in the presence of inactive tumour suppressors such as p53 or p16 (ref. 33) during long-term cell culture. Thus, the different genetic background and treatments might determine the different outcomes. Our genetic and biochemical data clearly show that in non-transformed primary MEFs, as well as embryonic liver cells, MKK7 is a crucial kinase for cell proliferation. In contrast, it has been shown that MKK7 is a negative regulator of haematopoietic cell proliferation[12,34]. The *in vitro* growth behaviours of haematopoietic cells are different from other cell types, and the role of MKK7–JNK in haematopoietic cells has only been studied under basal conditions. Thus, it would be interesting to determine the growth behaviours of such cells under conditions of stress, such as low population densities or altered serum condition. In addition, it is possible that MKK7 might regulate additional pathways.

One intriguing aspect of our results is that early passage *mkk7*$^{-/-}$ MEFs behave similarly to wild-type cells, but then rapidly down-regulate CDC2 expression and display premature senescence and defective proliferation. Similarly, proliferation of primary hepatocytes in *mkk7*$^{-/-}$ embryos seems to be normal in early foetal development, followed by downregulation of CDC2 and defective proliferation. In cell culture, it has been shown that conditions of stress, such as low serum or low cell densities, trigger premature senescence in wild-type fibroblasts and many other cell types[35]. Thus, it seems that under conditions of environmental stress and possibly during certain developmental processes such as liver formation, the MKK7–JNK–c-Jun pathway might function to upregulate CDC2 expression and maintain the proliferative state of the cells. Determination of cell fates by MKK7–JNK–c-Jun-induced CDC2 expression might explain why loss of MKK7 results in premature senescence and a G2/M cycle arrest, whereas the cells that express MKK7 undergo crisis at much later stages and predominantly arrest at G1 phase. Our results provide a molecular link between environmental stresses, premature senescence and G2/M cell-cycle progression. Whether MKK7–JNK-c-Jun signalling is involved in the regulation of molecules previously known to be involved in senescence needs to be determined. To investigate the connection to p53 (ref. 36) further, we generated *p53*$^{-/-}$*mkk7*$^{-/-}$ MEFs and observed rescue of CDC2 expression and cellular senescence, as well as restored proliferation. Thus, p53 is also important for the process. In addition, some other molecules controlled by the MKK7–JNK–c-Jun pathway might also be involved in the regulation of CDC2 expression at transcriptional, translational and post-translational levels, as it has been shown that *cdc2* transactivation is regulated by multiple mechanisms depending on cell types[37] and that c-Jun can control a variety of molecules such as E2F[19].

It has been suggested that the mechanisms regulating the cell cycle also have a role in apoptosis[38]. The induction of proteins that control G1/S transition in proliferating cells occurs in dying neurons[39], and G1 cyclin-dependent kinases seem to trigger neuronal cell death[40]. Moreover, E2F1-1 and CDK2 seem to control thymocyte apoptosis[41,42]. The G2/M cell-cycle regulator CDC2 induces phosphorylation of the BH3-only protein BAD and triggers neuronal apoptosis[43]. This notion is consistent with our results on the normal susceptibility to cell death in CDC2-expressing *mkk7*$^{-/-}$ MEFs, but the resistance to death triggers in *mkk7*$^{-/-}$ 3T3 cells that express low levels of CDC2. Furthermore, we showed that overexpression of constitutively active CDC2 in wild-type and *mkk7*$^{-/-}$ MEFs results in cell death (data not shown). Thus, regulation of CDC2 by stress kinases might be also involved in stress-kinase-regulated cell death. The role of JNKs in cell death has been controversial and is dependent on the experimental system used. Our results in MEF apoptosis experiments indicate that the MKK7–JNK–c-Jun pathway determines the molecular history of cells, and this is a critical determinant for cell death. Whether stress kinases also set the molecular switches for cell death susceptibility in other cell types remains to be determined.

Our results show that MKK7 is essential for embryogenesis and liver development. Loss of MKK7 in fibroblasts results in impaired proliferation, premature senescence and a G/2M cell-cycle arrest. We identified the G2/M kinase CDC2 as a molecular target for the MKK7–JNK–c-Jun signalling pathway. These data provide a new paradigm by which the MKK7–JNK–c-Jun signalling pathway couples developmental and environmental cues to proliferation, G2/M cycle arrest and cellular senescence. □

METHODS

Gene targeting. To disrupt the murine *mkk7* gene in embryonic stem cells, a portion of exon 9, including the phosphorylation motif, was replaced with a PGK-Neo cassette (see Supplementary information, Fig. S1a), as described previously[34]. *c-Jun* and *c-JunAA* mutant mice and MEFs have been described previously[13,19]. All mice were kept at the Ontario Cancer Institute and IMP animal facilities in accordance with institutional guidelines.

MEF and hepatocyte cultures. MEFs were prepared from E11.5 embryos and maintained in DMEM contatining 10% foetal calf serum (FCS). Cell proliferation in all MEFs was determined using WST-1 (Roche, Indianapolis, IN). The percentage of cells in each phase of the cell cycle was calculated with ModiFit software (Becton Dickinson, Oakville, Canada). Population doubling curves were determined using trypan-blue exclusion. For detection of apoptosis, MEFs were stained with annexin V/propidium iodide (PI) using an apoptosis detection kit (R&D Systems, Minneapolis, MN). For cell-cycle analysis, MEFs were fixed with 70% ethanol, labelled with PI and analysed by FACS. All samples were analysed by flow cytometry. Protein expression levels were determined using antibodies specific to p16, p21, cyclin D1, cyclin B1, MKK4, JNKs, p38-MAPK, ATF2, c-Jun, phospho-c-Jun, JunB, JunD (antibodies were purchased from Santa Cruz Biotechnology, Santa Cruz, CA), p53 (Novacastra, distributed by Vecter Laboratories, Burlingame, CA), CDC2 and ERK1/2 (Cell Signaling, Beverly, MA). For primary hepatocyte cultures, haematopoietic cells were depleted using antibodies to CD45 and TER119. The remaining parenchymal liver cells were cultured for 2 days, and cell proliferation was determined using WST-1 (Roche). *cdc2* mRNA expression was detected with a full-length CDC2 cDNA probe or RT-PCR. JNK activity in mouse embryonic liver was determined as described[44].

Expression assays. For ectopic gene expression, the retroviral vectors pBabe-puro, pBabe-puro-Flag-MKK7, pBabe-puro-MKK4, pBabe-puro-c-Jun or

pBabe-puro-CDC2 (wild-type) were transfected into a phoenix-E packaging cell line. MEFs were cultured in the supernatant of the packaging cells for 1 day and selected with 2.5 mg ml^{-1} puromycin for 2 days before recovery for a further 2 days. Empty pBabe-puro vectors did not have any detectable effect on the phenotype of MEFs.

Detection of senescent cells and cell staining. SA-β-gal staining was performed using a senescence staining kit (Cell Signaling). For Phalloidin–rhodamine/DAPI staining, SA-β-gal-stained cells were fixed, treated with 0.1% Triton X-100/3% skimmed milk/TBS and double-stained with phalloidin–rhodamine (Sigma, St Louis, MO) and DAPI (Molecular Probes, Eugene, OR). All SA-β-gal-positive cells had the typical flattened cell morphology determined by phalloidin/DAPI staining. Phospho-Histone H3 was determined using a phosphorylation (Ser 10)-specific antibody (Cell Signaling).

Promoter assays. The full-length CDC2 promoter was cloned from mouse genomic DNA using PCR, and the sequence was confirmed. The promoter constructs were transfected into Phoenix E cells or *mkk7*$^{+/-}$ and *mkk7*$^{-/-}$ MEFs, and luciferase activity was determined using a Luciferase Assay Kit (Promega, Madison, WI). For EMSAs, cell extracts were harvested from 5×10^6 cells according to standard protocols. Briefly, protein extracts (1 μg) were incubated in 20 μl binding buffer with end-labelled, double-stranded, oligonucleotide probes (consensus AP-1: 5'-CGCTTGATGACTCAGCCGGAA-3'; CDC2 promoter AP-1 site: 5'-AACAGAGCTCAAGAGTCAGTTGG-3'; mutant CDC2 promoter AP1 site: 5'-AACAGAGCTCAAGATCTAGTTGG-3') and fractionated on a 5% polyacrylamide gel. The binding buffer was: 10 mM Hepes-HCl at pH 7.9, 100 mM potassium chloride, 0.5 mM magnesium chloride, 0.1 mM EDTA, 0.5 mM dithiothreitol, 2 μg poly (dI-dC) and 10% glycerol. Chromatin immunoprecipitations (ChIPs) were performed as described[45]. The sequences of the ChIP primers were 5'-CTGTCACTTTGGTGGCTGGC-3' and 5'-TCCGACTCACGCCATACCTC-3' for *cdc2*; 5'-GTCAGCATCTAGCACACAGGTCC-3' and 5'-GAAATCCAGGTAGGGTTCCAGG-3' for *prim1*.

Kinase assays. To detect JNK and p38-MAPK activities, JNK proteins were immunoprecipitated at 4 °C using anti-JNK antibodies (C-17; Santa Cruz). Kinase activities were determined using glutathione *S*-transferase (GST)–c-Jun as a substrate in the presence of 50 μM γ-^{32}P-ATP. The amount of total JNK protein in the immunoprecipitated lysates were determined by Western blotting. cyclinB1/CDC2 kinase activities were determined by anti- cyclinB1 immunocomplex kinase assays using Histone H1 (HH1) as substrate.

Note: Supplementary Information is available on the Nature Cell Biology website.

ACKNOWLEDGMENTS

We thank J. Woodgett, L. Harrington, J. C. Zuniga-Pflucker, T. Schmitt, J. Joza, C. Krawczyk, E. Griffith, L. Barra, M. Crackower, U. Erickson, L. Zhang, H. Hara and M. Rangachari for discussion and reagents. T.W. is supported by the H15th fellowship of the Japan Society for the Promotion of Science. This work is supported by the National Cancer Institute of Canada (NCIC), the Institute of Molecular Biotechnology of the Austrian Academy of Sciences (IMBA), and the Jubilaeumsfonds of the Austrian National Bank.

COMPETING FINANCIAL INTERESTS

The authors declare that they have no competing financial interests.

Received 26 June 2003; accepted 28 January 2004
Published online at http://www.nature.com/naturecellbiology.

1. Chang, L. & Karin, M. Mammalian MAP kinase signalling cascades. *Nature* **410**, 37–40 (2001).
2. Seger, R. & Krebs, E. G. The MAPK signaling cascade. *FASEB J.* **9**, 726–735 (1995).
3. Tibbles, L. A. & Woodgett, J. R. The stress-activated protein kinase pathways. *Cell Mol. Life Sci.* **55**, 1230–1254 (1999).
4. Waskiewicz, A. J. & Cooper, J. A. Mitogen and stress response pathways: MAP kinase cascades and phosphatase regulation in mammals and yeast. *Curr. Opin. Cell Biol.* **7**, 798–805 (1995).
5. Davis, R. J. Signal transduction by the JNK group of MAP kinases. *Cell* **103**, 239–252 (2000).
6. Roovers, K. & Assoian, R. K. Integrating the MAP kinase signal into the G1 phase cell cycle machinery. *Bioessays* **22**, 818–826 (2000).
7. Johnson, G. L. & Lapadat, R. Mitogen-activated protein kinase pathways mediated by ERK, JNK, and p38 protein kinases. *Science* **298**, 1911–1912 (2002).
8. Kishimoto, H. *et al.* Different properties of SEK1 and MKK7 in dual phosphorylation of stress-induced activated protein kinase SAPK/JNK in embryonic stem cells. *J. Biol. Chem.* **278**, 16595–16601 (2003).
9. Wada, T. *et al.* Impaired synergistic activation of stress-activated protein kinase SAPK/JNK in mouse embryonic stem cells lacking SEK1/MKK4: different contribution of SEK2/MKK7 isoforms to the synergistic activation. *J. Biol. Chem.* **276**, 30892–30897 (2001).
10. Fleming, Y. *et al.* Synergistic activation of stress-activated protein kinase 1/c-Jun N-terminal kinase (SAPK1/JNK) isoforms by mitogen-activated protein kinase kinase 4 (MKK4) and MKK7. *Biochem J.* **352**, 145–154 (2000).
11. Nishina, H. *et al.* Defective liver formation and liver cell apoptosis in mice lacking the stress signaling kinase SEK1/MKK4. *Development* **126**, 505–516 (1999).
12. Dong, C. *et al.* JNK is required for effector T-cell function but not for T-cell activation. *Nature* **405**, 91–94 (2000).
13. Behrens, A., Sibilia, M. & Wagner, E. F. Amino-terminal phosphorylation of c-Jun regulates stress-induced apoptosis and cellular proliferation. *Nature Genet.* **21**, 326–329 (1999).
14. Behrens, A., Jochum, W., Sibilia, M. & Wagner, E. F. Oncogenic transformation by ras and fos is mediated by c-Jun N-terminal phosphorylation. *Oncogene* **19**, 2657–2663 (2000).
15. Tournier, C. *et al.* MKK7 is an essential component of the JNK signal transduction pathway activated by proinflammatory cytokines. *Genes Dev* **15**, 1419–1426 (2001).
16. Hochedlinger, K., Wagner, E. F. & Sabapathy, K. Differential effects of JNK1 and JNK2 on signal specific induction of apoptosis. *Oncogene* **21**, 2441–2445 (2002).
17. Tournier, C. *et al.* Requirement of JNK for stress-induced activation of the cytochrome *c*-mediated death pathway. *Science* **288**, 870–874 (2000).
18. Dimri, G. P. *et al.* A biomarker that identifies senescent human cells in culture and in aging skin *in vivo*. *Proc. Natl Acad. Sci. USA* **92**, 9363–9367 (1995).
19. Schreiber, M. *et al.* Control of cell cycle progression by c-Jun is p53 dependent. *Genes Dev* **13**, 607–619 (1999).
20. Sherwood, S. W., Rush, D., Ellsworth, J. L. & Schimke, R. T. Defining cellular senescence in IMR-90 cells: a flow cytometric analysis. *Proc. Natl Acad. Sci. USA* **85**, 9086–9090 (1988).
21. Paulson, J. R., Taylor, S. S., Lake, R. S. & Salzman, N. P. Phosphorylation of histones 1 and 3 and nonhistone high mobility group 14 by an endogenous kinase in HeLa metaphase chromosomes. *J. Biol. Chem.* **257**, 6064–6072 (1982).
22. Lake, R. S. & Salzman, N. P. Occurrence and properties of a chromatin-associated F1-histone phosphokinase in mitotic Chinese hamster cells. *Biochemistry* **11**, 4817–4826 (1972).
23. Bulavin, D. V. *et al.* Initiation of a G2/M checkpoint after ultraviolet radiation requires p38 kinase. *Nature* **411**, 102–107 (2001).
24. Shackelford, R. E., Kaufmann, W. K. & Paules, R. S. Cell cycle control, checkpoint mechanisms, and genotoxic stress. *Environ. Health Perspect.* **107**, 5–24 (1999).
25. Orren, D. K., Petersen, L. N. & Bohr, V. A. A UV-responsive G2 checkpoint in rodent cells. *Mol. Cell. Biol.* **15**, 3722–3730 (1995).
26. Toussaint, O. *et al.* Stress-induced premature senescence. Essence of life, evolution, stress, and aging. *Ann. NY Acad. Sci.* **908**, 85–98 (2000).
27. Th'ng, J. P. *et al.* The FT210 cell line is a mouse G2 phase mutant with a temperature-sensitive CDC2 gene product. *Cell* **63**, 313–324 (1990).
28. Arion, D., Meijer, L., Brizuela, L. & Beach, D. *cdc2* is a component of the M phase-specific histone H1 kinase: evidence for identity with MPF. *Cell* **55**, 371–378 (1988).
29. Okada, Y., Voznesensky, O., Herschman, H., Harrison, J. & Pilbeam, C. Identification of multiple *cis*-acting elements mediating the induction of prostaglandin G/H synthase-2 by phorbol ester in murine osteoblastic cells. *J. Cell. Biochem.* **78**, 197–209 (2000).
30. Dalton, S. Cell cycle regulation of the human cdc2 gene. *EMBO J.* **11**, 1797–1804 (1992).
31. Kovary, K. & Bravo, R. The jun and fos protein families are both required for cell cycle progression in fibroblasts. *Mol. Cell. Biol.* **11**, 4466–4472 (1991)
32. Kennedy, N. J. *et al.* Suppression of Ras-stimulated transformation by the JNK signal transduction pathway. *Genes Dev.* **17**, 629–637 (2003).
33. Serrano, M., Lin, A. W., McCurrach, M. E., Beach, D. & Lowe, S. W. Oncogenic ras provokes premature cell senescence associated with accumulation of p53 and p16INK4a. *Cell* **88**, 593–602 (1997).
34. Sasaki, T. *et al.* The stress kinase mitogen-activated protein kinase kinase (MKK)7 is a negative regulator of antigen receptor and growth factor receptor-induced proliferation in hematopoietic cells. *J. Exp. Med.* **194**, 757–768 (2001).
35. Didinsky, J. B. & Rheinwald, J. G. Failure of hydrocortisone or growth factors to influence the senescence of fibroblasts in a new culture system for assessing replicative lifespan. *J. Cell. Physiol.* **109**, 171–179 (1981).
36. Wynford-Thomas, D. p53: guardian of cellular senescence. *J. Pathol.* **180**, 118–121 (1996).
37. Sugarman, J. L., Schonthal, A. H. & Glass, C. K. Identification of a cell-type-specific and E2F-independent mechanism for repression of cdc2 transcription. *Mol. Cell. Biol.* **15**, 3282–3290 (1995).
38. King, K. L. & Cidlowski, J. A. Cell cycle and apoptosis: common pathways to life and death. *J. Cell. Biochem.* **58**, 175–180 (1995).
39. Freeman, R. S., Estus, S. & Johnson, E. M. Jr. Analysis of cell cycle-related gene expression in postmitotic neurons: selective induction of cyclin D1 during programmed cell death. *Neuron* **12**, 343–355 (1994).
40. Park, D. S. *et al.* cyclin-dependent kinases participate in death of neurons evoked

by DNA-damaging agents. *J. Cell Biol.* **143**, 457–467 (1998).
41. Hakem, A., Sasaki, T., Kozieradzki, I. & Penninger, J. M. The cyclin-dependent kinase Cdk2 regulates thymocyte apoptosis. *J. Exp. Med.* **189**, 957–968 (1999).
42. Field, S. J. *et al.* E2F-1 functions in mice to promote apoptosis and suppress proliferation. *Cell* **85**, 549–561 (1996).
43. Konishi, Y., Lehtinen, M., Donovan, N. & Bonni, A. Cdc2 phosphorylation of BAD links the cell cycle to the cell death machinery. *Mol. Cell* **9**, 1005–1016 (2002).
44. Watanabe, T. *et al.* SEK1/MKK4-mediated SAPK/JNK signaling participates in embryonic hepatoblast proliferation via a pathway different from NF-κB-induced anti-apoptosis. *Dev. Biol.* **250**, 332–347 (2002).
45. Weinmann, A. S., Bartley, S. M., Zhang, T., Zhang, M. Q. & Farnham, P. J. Use of chromatin immunoprecipitation to clone novel E2F target promoters. *Mol. Cell Biol.* **21**, 6820–6832 (2001).

THE JOURNAL OF BIOLOGICAL CHEMISTRY
Vol. 279, No. 3, Issue of January 16, pp. 1621–1626, 2004
Printed in U.S.A.

Stress Induces Mitochondria-mediated Apoptosis Independent of SAPK/JNK Activation in Embryonic Stem Cells*

Received for publication, September 17, 2003, and in revised form, October 24, 2003
Published, JBC Papers in Press, October 29, 2003, DOI 10.1074/jbc.M310335200

Gen Nishitai‡, Nao Shimizu‡, Takahiro Negishi‡, Hiroyuki Kishimoto‡, Kentaro Nakagawa‡, Daiju Kitagawa‡, Tomomi Watanabe‡, Haruka Momose‡, Shinya Ohata‡, Shuhei Tanemura‡, Satoshi Asaka‡, Junko Kubota‡, Ryota Saito‡, Hiroki Yoshida§, Tak W. Mak¶, Teiji Wada¶, Josef M. Penninger¶, Noriyuki Azuma‖, Hiroshi Nishina‡, and Toshiaki Katada‡**

From the ‡Department of Physiological Chemistry, Graduate School of Pharmaceutical Sciences, University of Tokyo, Tokyo 113-0033, Japan, the §Department of Biomolecular Sciences, Saga Medical School, Saga 849-8501, Japan, the ¶University Health Network, Departments of Medical Biophysics and Immunology, the University of Toronto, Toronto, Ontario M5G 2C1, Canada, and the ‖Department of Ophthalmology, National Center for Child Health and Development, 2-10-1, Okura, Setagaya-ku, Tokyo 157-8535, Japan

SAPK/JNK, which belongs to the family of mitogen-activated protein kinase (MAPK), is activated by many types of cellular stresses or extracellular signals and is involved in embryonic development, immune responses, and cell survival or apoptosis. However, the physiological roles of SAPK/JNK in the signaling of stress-induced apoptosis are still controversial. To evaluate the precise function, SAPK/JNK-inactivated mouse embryonic stem (ES) cells were generated by disrupting genes of the MAPK activators, SEK1 and MKK7. Although SAPK/JNK activation by various stresses was completely abolished in *sek1*$^{-/-}$ *mkk7*$^{-/-}$ ES cells, apoptotic responses including DNA fragmentation and caspase 3 activation still occurred normally, which displays a sharp contrast to *apaf1*$^{-/-}$ ES cells exhibiting profound defects in the mitochondria-dependent apoptosis. These normal apoptotic responses without SAPK/JNK activation were also observed in fibroblasts derived from *sek1*$^{-/-}$ *mkk7*$^{-/-}$ ES cells. Instead, interleukin-1β (IL-1β)-induced IL-6 gene expression was greatly suppressed in *sek1*$^{-/-}$ *mkk7*$^{-/-}$ fibroblasts. These results clearly show that SAPK/JNK activation is responsible for the inflammatory cytokine-induced gene expression but not essentially required for the mitochondria-dependent apoptosis at least in ES or fibroblast-like cells, which are prototypes of all cell lineages.

Apoptosis or programmed cell death is critical for many biological events such as embryonic development, immune responses, and tissue homeostasis in multicellular organisms. In mammalian cells, apoptotic signaling cascades can be divided into two broad categories: the intrinsic (mitochondria-dependent) and the extrinsic (death receptor-mediated) pathways. The initiation of mitochondria-dependent pathway requires a change in the organella membrane permeability that is prevented by anti-apoptotic molecules such as Bcl-2 and Bcl-X_L and promoted by pro-apoptotic molecules including Bax and Bak, and the permeability change results in the release of mitochondrial proteins. One of the released proteins, cytochrome *c*, associates with Apaf1 and caspase 9 to activate the effector caspase 3 (1, 2). Cellular stresses such as UV irradiation and heat shock mediate apoptosis through the mitochondria-dependent pathway (3). However, upstream signaling that regulates the pro-apoptotic molecules remains to be elucidated.

Stress-activated protein kinase/c-Jun N-terminal kinase (SAPK/JNK),[1] which belongs to the family of mitogen-activated protein kinase (MAPK), is activated not only by many types of cellular stresses including UV irradiation, heat shock, cisplatinum, etoposide, thapsigargin, and tunicamycin but also by inflammatory cytokines, interleukin-1β (IL-1β), and tumor necrosis factor α (TNF-α). The activated SAPK/JNK phosphorylates a number of substrates including the c-Jun component of the activator protein-1 transcription factor to regulate gene expression for the stress responses. Activation of SAPK/JNK requires the dual phosphorylation of Tyr and Thr residues located in a Thr-Pro-Tyr motif of the MAPK, and two kinases, SEK1 (also known as MKK4) and MKK7 (SEK2), are responsible for the phosphorylation (4–6). SEK1 and MKK7 preferentially phosphorylate the Tyr and Thr residues of SAPK/JNK, respectively (7). Interestingly, the Tyr phosphorylation by SEK1 is sequentially followed by the Thr phosphorylation by MKK7 in stress-stimulated mouse embryonic stem (ES) cells (8, 9).

Targeted gene-disruption experiments in mice demonstrate that both SEK1 and MKK7 are required for embryonic development. *Sek1*$^{-/-}$ embryos die between embryonic day 10.5 (E10.5) and E12.5 with impaired liver formation and massive apoptosis (10, 11). We have recently shown that SEK1-mediated SAPK/JNK pathway downstream TNF-α receptor 1 participates in embryonic hepatoblast proliferation and survival via a pathway different from NF-κB-induced anti-apoptosis. On the other hand, *mkk7*$^{-/-}$ embryos die between E11.5 and 12.5 with similar defects in liver formation. These results indicate that SAPK/JNK activation mediated through SEK1 *plus* MKK7 plays indispensable roles in hepatoblast proliferation and survival during mouse embryogenesis (12).

* This work was supported in part by research grants from the Ministry of Education, Science, Sports, and Culture and the Ministry of Health, Labor and Welfare of Japan. The costs of publication of this article were defrayed in part by the payment of page charges. This article must therefore be hereby marked "*advertisement*" in accordance with 18 U.S.C. Section 1734 solely to indicate this fact.

** To whom correspondence should be addressed: Dept. of Physiological Chemistry, Graduate School of Pharmaceutical Sciences, University of Tokyo, 7-3-1 Hongo, Bunkyo-ku, Tokyo 113-0033, Japan. Tel.: 81-3-5841-4754; Fax: 81-3-5841-4751; E-mail: nishina@mol.f.u-tokyo.ac.jp.

[1] The abbreviations used are: SAPK/JNK, stress-activated protein kinase/c-Jun N-terminal kinase; MAPK, mitogen-activated protein kinase; MKK, MAPK kinase; SEK, stress-activated protein kinase/extracellular signal-regulated kinase kinase; ES, embryonic stem; MEF, mouse embryonic fibroblast; IL, interleukin; TNF-α, tumor necrosis factor α; E, embryonic day; ERK, extracellular signal-regulated kinase.

However, the physiological role of SAPK/JNK activation in cell survival and apoptosis is still controversial, being suggested to have an anti-apoptotic, pro-apoptotic, or no function in these processes (13). Mice lacking both JNK1 and JNK2 ($Jnk1^{-/-}$ $Jnk2^{-/-}$) die around E11 with defective neural tube morphogenesis and altered apoptosis (14, 15). These results assign both pro- and anti-apoptotic functions to JNK1 and JNK2 in the development. It also appears that the SAPK/JNK pathway functions in a manner dependent on the types of cells and stimulus, and its different components can sometimes play opposing roles in apoptosis. The most convincing evidence to date that shows that the involvement of SAPK/JNK activation in pro-apoptotic function comes from $Jnk1^{-/-}$ $Jnk2^{-/-}$ and $mkk4^{-/-}$ $mkk7^{-/-}$ mouse embryonic fibroblasts (MEFs). Both $Jnk1^{-/-}$ $Jnk2^{-/-}$ and $mkk4^{-/-}$ $mkk7^{-/-}$ MEFs exhibited profound defects in stress-induced apoptosis (16, 17). Furthermore, it has been reported that active JNK causes the release of apoptogenic factors such as cytochrome *c* and Smac from isolated mitochondria in a cell-free system (18, 19). These results strongly indicate that the SAPK/JNK activation directly regulates mitochondria-dependent apoptosis in pro-apoptotic direction.

To evaluate the exact role of SAPK/JNK activation in mitochondria-dependent apoptosis, we here utilized mouse ES cells in terms of the following advantages. 1) ES cells are a prototype of all cell lineages and can be differentiated into MEF-like cells with retinoic acid. 2) ES cells do not express death receptors including Fas and TNF-α receptor 1 but have stress-induced mitochondria-dependent apoptotic pathway. 3) The molecular mechanism of SAPK/JNK activation is well characterized in ES cells. The present results clearly show that SAPK/JNK activation is not required for the stress-induced mitochondria-dependent apoptosis in ES and MEF-like cells. Instead, we found that IL-1-induced IL-6 gene expression was greatly impaired in MEF derived from $sek1^{-/-}$ $mkk7^{-/-}$ ES cells.

EXPERIMENTAL PROCEDURES

Cell Culture and Materials—The murine ES cell line E14K (wild type) was maintained in Dulbecco's modified Eagle's medium supplemented with 15% fetal calf serum and leukemia inhibitory factor as described previously (20). The generation of $apaf1^{-/-}$ ES cells was described previously (3). $Sek1^{-/-}$ $mkk7^{-/-}$ ES cells were newly generated as described in Fig. 2. MEF-like cells are prepared from ES cells by culture with 10 μM retinoic acid for 14 days without leukemia inhibitory factor. For thermotolerance, cells were incubated at 44 °C for 10 min and further cultured for 6 h.

Antibodies against SAPK/JNK1 (C-17 and FL), p38 (C-20), ERK2, and Bax were purchased from Santa Cruz Biotechnology, Inc. Anti-phospho-SAPK/JNK (number 9251) and anti-phospho-p38 (number 9211) antibodies were from New England BioLabs, Inc. Anti-mitochondrial heat shock protein 70 was from Affinity BioReagents. Rat anti-SEK1 (KN-001) and anti-MKK7 (KN-004) antibodies applicable to immunoprecipitation and immunoblotting were prepared in our laboratory (8). SB203580 and SP600125 were from Calbiochem and Biomol, respectively. Adenovirus-encoding Cre recombinase (number 1748) was from DNA Bank, BioResource Center, RIKEN (Ibaraki, Japan) (21).

Generation of ES Cells Lacking Both SEK1 and MKK7—sek1 and *mkk7* genes were disrupted as shown in Fig. 2*a*. Steps 1 and 2 were done by using a *sek1* (neomycin)-targeting vector and gene-dosage effect, respectively (20). Steps 3 and 4 were performed by using a *mkk7* (loxP-hygromycin)-targeting vector and an adenovirus-encoding Cre recombinase, respectively (9, 21). Step 5 was done by using a novel *mkk7* (puromycin)-targeting vector as shown in Fig. 2*a*.

Assay of SAPK/JNK Activity—ES cells were plated at 1.5×10^6 cells/35-mm dish and cultured for overnight. The cells were stimulated by anisomycin (Sigma, 5 μg/ml), cisplatinum (Sigma, 50 μM), etoposide (Sigma, 2 μg/ml), thapsigargin (Sigma, 200 nM), tunicamycin (Sigma, 10 μg/ml), UV (1 kJ/m^2, UV Stratalinker 1800, Stratagene), and heat shock (44 °C for 20 min). SAPK/JNK proteins were immunoprecipitated at 4 °C for 2 h using the anti-SAPK/JNK antibody (C-17, Santa Cruz Biotechnology, Inc.). The SAPK/JNK activity in the precipitated fractions was measured with glutathione *S*-transferase-c-Jun as an *in vitro* substrate in the presence of 60 μM [γ-^{32}P]ATP (8, 9). The amount of the precipitated SAPK/JNK that had been monitored by immunoblotting with the anti-SAPK/JNK (FL) antibody was almost constant in a series of the present experiments.

Immunoprecipitation and Immunoblotting—ES cells (2×10^6 cells) were suspended at 4 °C in 0.2 ml of a lysis buffer consisting of 1% Nonidet P-40, 80 mM Tris-HCl (pH 7.5), 10 mM EDTA, and 4 μg/ml aprotinin. The cell lysates were incubated for 30 min and centrifuged at 15,000 rpm for 15 min. The supernatants were analyzed by SDS-PAGE and immunoblotting. Proteins were transferred to a polyvinylidene difluoride membrane (Bio-Rad) and probed with antibodies against anti-SAPK/JNK1, anti-ERK2, anti-p38, and anti-phospho-SAPK/JNK. The bands were visualized by SuperSignal West Pico chemiluminescent substrate for the development of immunoblots utilizing a horseradish peroxidase-conjugated second antibody according to the manufacturer's instructions (Pierce). For detection of phospho-p38, cells were lysed directly in Laemmli sample buffer and sonicated by Ultrasonic Disruptor (TOMY) followed by SDS-PAGE and immunoblotting. Endogenous SEK1 and MKK7 were immunoprecipitated with anti-SEK1 (KN-001) and anti-MKK7 (KN-004) and detected with anti-SEK1 (C-20) and anti-MKK7 (T-19) antibodies, respectively (8, 9).

DNA Fragmentation Assay—ES cells (2×10^6 cells), which had been attached to and detached from culture dishes after stimuli, were collected by means of incubation with trypsin/EDTA and centrifugation, respectively. The cells were mixed, washed twice with phosphate-buffered saline, and collected by centrifugation. After removing the supernatants, the cells were lysed in 0.33 ml of a buffer consisting of 5 mM Tris-HCl (pH 7.4), 20 mM EDTA, and 0.5% Triton X-100. After centrifugation at 27,000 $\times$ *g* for 20 min at 4 °C to remove nuclei and insoluble fraction, the cell lysates were subjected to phenol extraction and ethanol precipitation for DNA purification. The precipitated DNA was suspended in 20 μl of H_2O and treated with 50 μg/ml RNase for 30 min at 37 °C. The DNA samples (10 μl) were subjected to electrophoresis on 2% agarose gels and visualized by a UV illuminator (22).

Assay of Caspase 3 Activity—ES cells were harvested as described above and washed twice with phosphate-buffered saline. The cells, after being resuspended in 50 μl of a buffer consisting of 10 mM Tris-HCl (pH 7.5), 5 mM dithiothreitol, and 1 mM phenylmethanesulfonyl fluoride, were frozen in liquid nitrogen and thawed at 37 °C three times. The cell lysates (50 μg) were incubated at 37 °C for 1 h with 20 μM acetyl-Asp-Glu-Val-Asp α-(4-methyl-coumaryl-7-amide) (DEVD-MCA; Peptide Institute, Inc.) in the final volume of 50 μl in 20 mM Hepes-NaOH (pH 7.4), 2 mM dithiothreitol, and 10% glycerol. The reaction was terminated by adding 450 μl of ice-cold H_2O, and substrate cleavage leading to the release of free MCA was monitored (excitation 355 nm and emission 460 nm) at room temperature (22).

Sub-G_1 Assay—For flow-cytometric analysis, cells were first fixed with 70% ethanol and further incubated with 10 μg/ml RNase A at 37 °C for 1 h. The cells were stained in a solution (50 μg of propidium iodide/ml, 0.1% sodium citrate, and 0.1% Nonidet P-40) for 30 min at 4 °C. The apoptotic sub-G_1 population was determined by FACScan flow cytometer (BD Biosciences) with Cell Quest software (23).

Subcellular Fractionation—ES cells (1×10^7 cells) were harvested by cell scraper (SUMILON) and washed twice with phosphate-buffered saline. The cells, after being resuspended in 100 μl of buffer A consisting of 250 mM sucrose, 20 mM HEPES-KOH (pH 7.4), 10 mM KCl, 1.5 mM Na-EGTA, 1.5 mM Na-EDTA, 1 mM $MgCl_2$, 1 mM dithiothreitol, and 2 μg/ml aprotinin, were homogenized 10 strokes by a 27-gauge syringe. After homogenization, cells were centrifuged at 600 $\times$ *g* for 10 min at 4 °C to remove nuclei, unbroken cells, and large debris. Supernatants containing mitochondria were transferred to a new tube and further centrifuged at 10,000 $\times$ *g* for 10 min at 4 °C. Mitochondrial pellets were washed in 100 μl of buffer A followed by centrifugation at 10,000 $\times$ *g* for 10 min at 4 °C and lysed in 1.5$\times$ Laemmli sample buffer. The samples (10 μl) were analyzed by SDS-PAGE, and immunoblotting was probed with the anti-Bax and mitochondrial heat shock protein 70 antibodies.

Northern Blotting—Total RNA was prepared from differentiated ES cells by TRIzol reagent (Invitrogen), separated by formamide agarose gel, and transferred to a Hybond-XL (Amersham Biosciences). IL-6 and β-actin were detected by Northern blotting using the specific DNA probes. The cDNA fragments corresponding to mouse IL-6 and β-actin were amplified using the following primers: IL-6, 5'-ATG AAG TTC CTC TCT GCA AGA GAC T-3' and 5'-CAC TAG GTT TGC CGA GTA GAT CTC-3', and β-actin, 5'-CAT CAC TAT TGG CAA CGA GC-3' and 5'-ACG CAG CTC AGT AAC AGT CC-3'.

All of the experiments were repeated at least three times with different batches of the cell samples, and the results were fully reproduc-

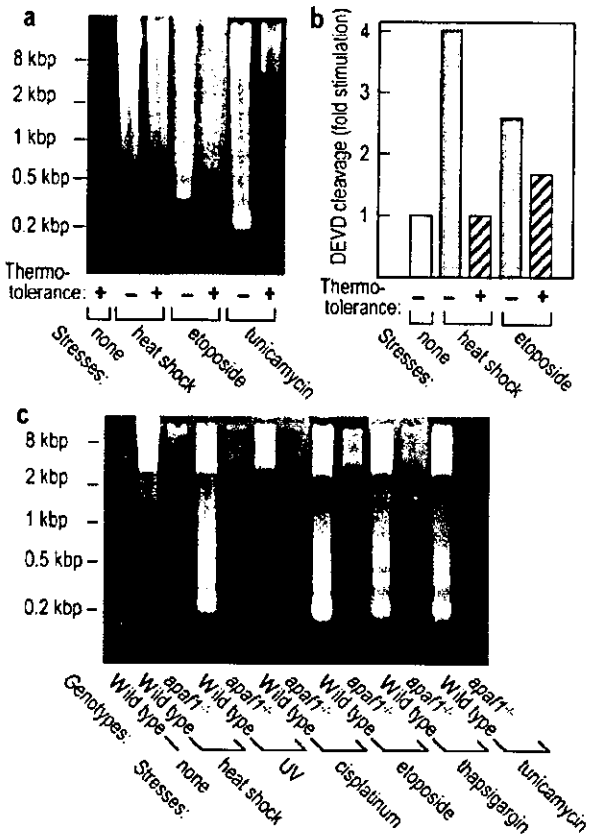

FIG. 1. **Characterization of stress-induced apoptosis in ES cells.** Wild-type ES cells were treated with (+) or without (−) heat shock at 44 °C for 10 min (*thermotolerance*), incubated for 6 h, and stimulated with the indicated stresses for 12 h. *a*, agarose-gel electrophoresis of DNA fragmentation. *b*, caspase 3 activation measured by DEVD cleavage. *c*, wild-type and *apaf1*$^{-/-}$ ES cells were stimulated with heat shock (44 °C for 20 min), UV (20 J/m^2), cisplatinum (50 μM), etoposide (2 μg/ml), thapsigargin (200 nM), or tunicamycin (10 μg/ml) and further incubated for 12 h. DNA fragmentation was measured by agarose-gel electrophoresis. The data shown are representative of three independent experiments.

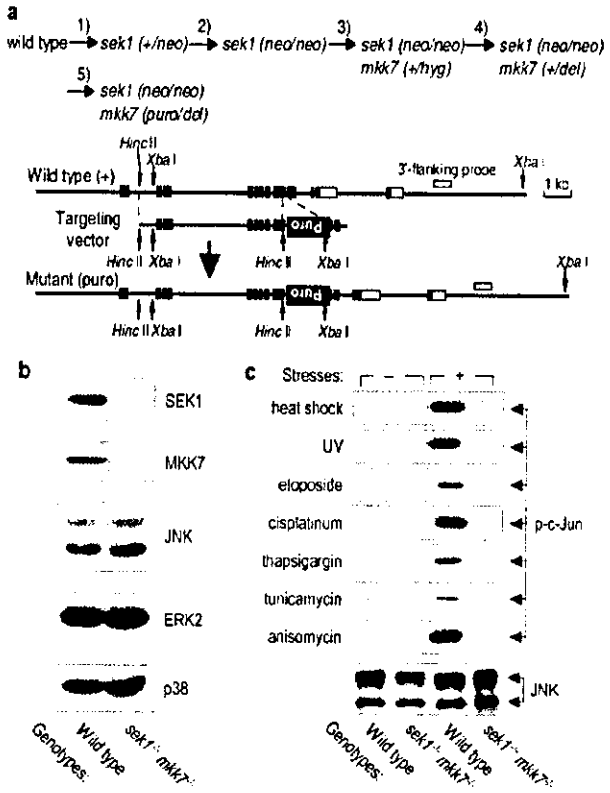

FIG. 2. **Targeted gene disruption of both *sek1* and *mkk7* in mouse ES cells.** *a*, flow chart of the disruption of *sek1* and *mkk7* genes and a novel *mkk7* (puromycin)-targeting vector. The genomic *mkk7* 3′-flanking probe used for Southern blotting is indicated as *gray boxes*, and the predicted structures of targeted alleles are shown as *puro*. Restriction enzymes used for the vector construction (HincII) and genomic Southern blotting (XbaI) are indicated by *arrows*. See "Experimental Procedures" for further explanation. *b*, Western blot analysis of SEK1, MKK7, JNK, ERK2, and p38 in wild-type and *sek1*$^{-/-}$ *mkk7*$^{-/-}$ ES cells. *c*, SAPK/JNK activity in wild-type and *sek1*$^{-/-}$ *mkk7*$^{-/-}$ ES cells. ES cells were stimulated with heat shock (44 °C for 20 min), UV (1 kJ/m^2 for 20 min), etoposide (2 μg/ml for 8 h), cisplatinum (50 μM for 8 h), thapsigargin (200 nM for 30 min), tunicamycin (10 μg/ml for 30 min), or anisomycin (5 μg/ml for 30 min). The amounts of JNK, ERK2, and p38 in *sek1*$^{-/-}$ *mkk7*$^{-/-}$ ES cells were comparable with those in wild-type cells.

ible. Hence, most of the data shown are representative of several independent experiments.

RESULTS

Various Stresses Induce Apoptosis through Mitochondria in Mouse ES Cells—We first investigated the thermotolerance effect on apoptosis in ES cells, which protects cells against successive stress by the pretreatment of mild heat shock. For this mechanism, a recent study revealed that HSP70 and HSP27 induced by thermotolerance suppress mitochondria-dependent apoptosis by directly associating with Apaf1 and cytochrome *c* and blocking the assembly of a functional apoptosome (24–26). As shown in Fig. 1, various stresses could induce DNA ladder formation (Fig. 1*a*) and caspase 3 activation, which was measured by DEVD cleavage (Fig. 1*b*) in wild-type ES cells. However, these apoptotic responses were markedly attenuated by the thermotolerance treatment. To confirm the involvement of Apaf1 in the stress-induced apoptosis, ES cells lacking Apaf1 (*apaf1*$^{-/-}$) (3) were subjected to the same experiments. As shown in Fig. 1*c*, apoptosis in response to various stresses including heat shock, UV, cisplatinum, etoposide, thapsigargin, and tunicamycin was almost completely blocked in *apaf1*$^{-/-}$ ES cells. These results clearly show that the stress-induced apoptosis is mediated through mitochondria in ES cells.

Stress-induced SAPK/JNK Activation Is Impaired in ES Cells Lacking both MKK4 and MKK7—To examine the role of SAPK/JNK activation in the stress-induced and mitochondria-dependent apoptosis, ES cells lacking both MKK4 and MKK7 were generated. For generation of the null mutant, we constructed a novel *mkk7*-targeting vector containing puromycin-resistant cassette (Fig. 2*a*), and disrupted *sek1* and *mkk7* genes as described previously (9, 20). The mutant *sek1(neo/neo) mkk7(puro/del)* clones thus generated lack both SEK1 and MKK7 completely (Fig. 2*b*), and these clones are used as *sek1*$^{-/-}$ *mkk7*$^{-/-}$ ES cells in this study. As shown in Fig. 2*c*, not only stress-induced activation but also the basal level of SAPK/JNK was completely lost in *sek1*$^{-/-}$ *mkk7*$^{-/-}$ ES cells.

Stress-induced Apoptosis Is Still Observed in sek1$^{-/-}$ *mkk7*$^{-/-}$ *ES Cells*—To examine the SAPK/JNK-inactivation effect, various apoptotic responses including caspase 3 activation, DNA fragmentation, and sub-G_1 population were further analyzed in *sek1*$^{-/-}$ *mkk7*$^{-/-}$ ES cells in comparison with wild-type and *apaf1*$^{-/-}$ ES cells (Fig. 3). Surprisingly, the apoptotic responses were still observed clearly in *sek1*$^{-/-}$ *mkk7*$^{-/-}$ ES cells at the same levels as wild-type ES cells. In sharp contrast, such responses were almost completely abolished in *apaf1*$^{-/-}$

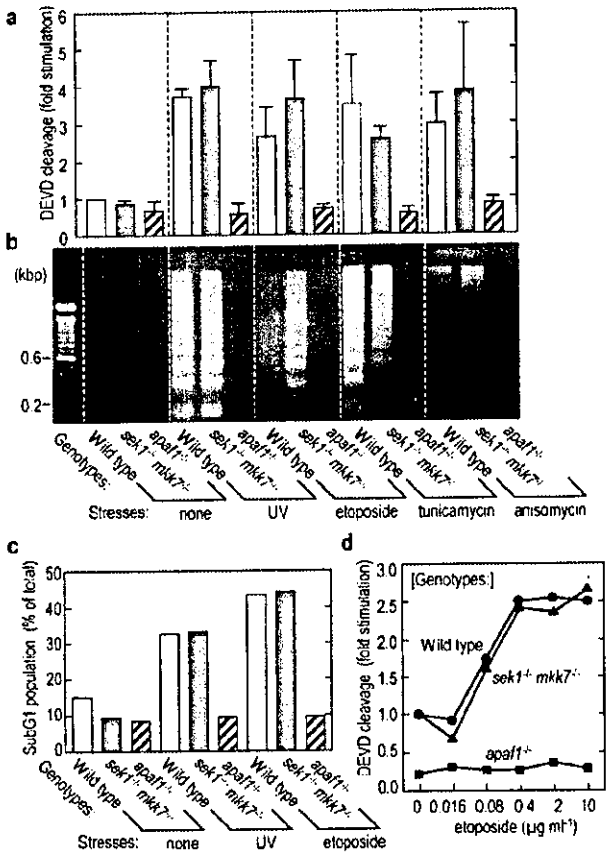

FIG. 3. **Stress-induced apoptosis in wild-type, *sek1*$^{-/-}$ *mkk7*$^{-/-}$, and *apaf1*$^{-/-}$ ES cells.** ES cells were stimulated with UV (20 J/m^2), etoposide (2 μg/ml), tunicamycin (10 μg/ml), or anisomycin (5 μg/ml) and further incubated for 12 h, and caspase 3 activation (*a*), DNA fragmentation (*b*), and sub-G_1 population (*c*) were measured. ES cells were stimulated with the indicated concentrations of etoposide, and caspase 3 activation (*d*) was measured.

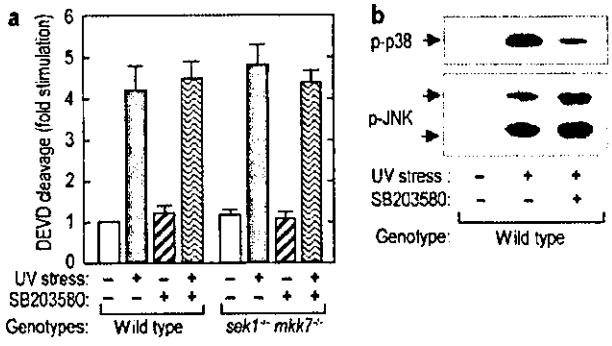

FIG. 4. **Effect of p38 inhibition on stress-induced apoptosis in ES cells.** *a*, ES cells were incubated with (+) or without (−) 10 μM SB203580 for 1 h, stimulated with UV (20 J/m^2), and further incubated for 12 h. UV-induced apoptosis was estimated by caspase 3 activation. *b*, ES cells were stimulated with UV (1 kJ/m^2 for 30 min) in the presence (+) or absence (−) of 10 μM SB203580, and active forms of p38 and JNK were detected by immunoblotting with anti-phospho-p38 and anti-phospho-JNK antibodies.

cells. The dose dependence and time course of etoposide-induced apoptosis were also the same between *sek1*$^{-/-}$ *mkk7*$^{-/-}$ and wild-type ES cells (Fig. 3*d* and data not shown). Thus, the SAPK/JNK inactivation appears to exert no influence on the stress-induced apoptosis in ES cells.

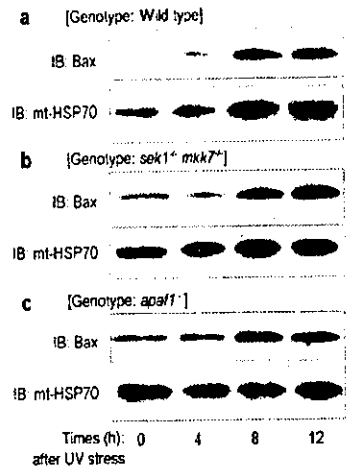

FIG. 5. **Stress-induced Bax translocation in wild-type, *sek1*$^{-/-}$ *mkk7*$^{-/-}$, and *apaf1*$^{-/-}$ ES cells.** ES cells were stimulated with UV (200 J/m^2) and further incubated for 4, 8, and 12 h. Mitochondrial membranes were prepared and immunoblotted (*IB*) with anti-Bax and anti-mitochondrial heat shock protein 70 (*mt-HSP70*) antibodies.

No Involvement of p38 Activation in Stress-induced Apoptosis in sek1$^{-/-}$ *mkk7*$^{-/-}$ *ES Cells*—Since it has been reported that another stress-responsive MAPK, p38, plays a pro-apoptotic role under certain conditions (27), we examined the effect of a p38 inhibitor (SB203580) on UV stress-induced apoptosis. As shown in Fig. 4, SB203580 markedly suppressed the phosphorylation of p38 but failed to inhibit the stress-induced apoptosis both in wild-type and *sek1*$^{-/-}$ *mkk7*$^{-/-}$ ES cells. These results indicate that p38 activation is not responsible for the stress-induced apoptosis in ES cells.

No Requirement of SAPK/JNK Activation for Bax Translocation in ES Cells—The above results shown in Figs. 1–3 suggest that SAPK/JNK activation is not required for mitochondria-dependent apoptosis in ES cells. We next measured the initiation step of mitochondria-dependent apoptosis, the translocation of Bax from cytoplasm to mitochondrial membranes, since it has been recently reported that SAPK/JNK activation potentiates Bax-dependent apoptosis in neuronal cells (28). Fig. 5 shows the time courses of the Bax translocation in response to UV irradiation in *sek1*$^{-/-}$ *mkk7*$^{-/-}$, *apaf1*$^{-/-}$, and wild-type ES cells. There were no significant differences among the three types of ES cells. These results clearly show that SAPK/JNK activation is not required for the initiation of mitochondria-dependent apoptosis in ES cells.

Stress-induced Apoptosis Is Also Observable in sek1$^{-/-}$ *mkk7*$^{-/-}$ *MEF-like Cells*—Since it has recently been reported that SAPK/JNK is crucial for stress-induced apoptosis in MEF (16, 17), ES cells were treated with retinoic acid and induced to differentiate into MEF-like cells. As shown in Fig. 6, stress-induced apoptosis measured by DNA fragmentation was also observed at the same level between *sek1*$^{-/-}$ *mkk7*$^{-/-}$ and wild-type MEF-like cells as had been observed in non-differentiated ES cells (see Fig. 3*b*). These results indicate that SAPK/JNK inactivation does not exert its influence on the stress-induced apoptosis in MEF-like cells as well as in ES cells.

IL-1-induced IL-6 Gene Expression Is Impaired in sek1$^{-/-}$ *mkk7*$^{-/-}$ *MEF-like Cells*—To understand the physiological role of SAPK/JNK activation in ES or MEF-like cells, we examined gene expression induced by an inflammatory cytokine, IL-1. As shown in Fig. 7*a*, IL-6 mRNA was induced at 1 and 6 h in wild-type cells. However, this induction was greatly inhibited in *sek1*$^{-/-}$ *mkk7*$^{-/-}$ MEF-like cells, which express IL-1 receptors. Furthermore, the IL-1-dependent IL-6 expression

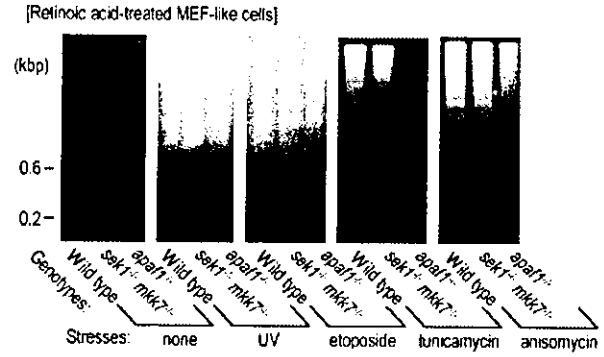

FIG. 6. **Stress-induced apoptosis in wild-type, *sek1*$^{-/-}$ *mkk7*$^{-/-}$, and *apaf1*$^{-/-}$ MEF-like cells.** ES cells were treated with 10 μM retinoic acid for 14 days and differentiated into MEF-like cells. The cells were stimulated UV (200 J/m^2), etoposide (20 μg/ml), tunicamycin (50 μg/ml), or anisomycin (50 μg/ml) and further incubated for 20 h. UV-induced apoptosis was measured by DNA fragmentation.

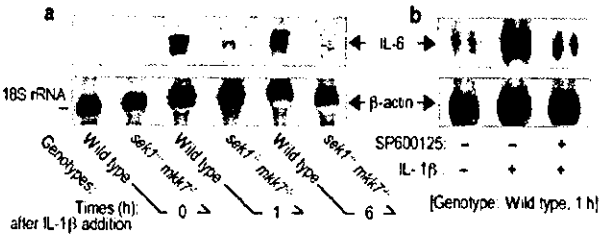

FIG. 7. **IL-1-induced IL-6 gene expression is impaired in *sek1*$^{-/-}$ *mkk7*$^{-/-}$ MEF-like cells.** *a*, wild-type and *sek1*$^{-/-}$ *mkk7*$^{-/-}$ MEF-like cells were stimulated with 100 ng/ml IL-1β for 1 and 6 h. *b*, wild-type MEF-like cells were incubated with (+) or without (−) 50 μM SP600125 for 1 h and further stimulated with IL-1β for 1 h. Total RNAs were prepared and applied on agarose gel. IL-6 and β-actin mRNAs were detected by Northern blot analysis.

was greatly suppressed by adding the JNK inhibitor SP600125 in wild-type MEF-like cells (Fig. 7*b*). Thus, SAPK/JNK activation appears to play an important role in the inflammatory cytokine-induced gene expression rather than the apoptotic responses at least in ES or MEF-like cells.

DISCUSSION

In the previous study, we have reported that *sek1*$^{-/-}$ thymocytes are susceptible to Fas/CD95- and CD3-mediated apoptosis and that apoptosis is increased in *sek1*$^{-/-}$ hepatoblasts (11, 20). These results indicate that SAPK/JNK activation is involved in cell survival. However, it has been reported that *Jnk1*$^{-/-}$ *Jnk2*$^{-/-}$ and *mkk4*$^{-/-}$ *mkk7*$^{-/-}$ MEFs are resistant to UV-induced apoptosis (16, 17). Furthermore, there are many other reports supporting the involvement of SAPK/JNK activation both in cell survival and in apoptosis. Thus, the role of SAPK/JNK in cell survival and apoptosis is still controversial (13). Our present results do not support the concept that "SAPK/JNK activation is required for the stress-induced and mitochondria-dependent apoptosis" (4, 16, 17), at least in ES and MEF-like cells, based on the following findings.

First, SAPK/JNK activation is completely dependent on the existence of both SEK1 and MKK7 in mouse ES cells in which stress-induced apoptosis is mediated through mitochondria (Fig. 1). The mutant *sek1*$^{-/-}$ *mkk7*$^{-/-}$ ES cells had a defect in the SAPK/JNK activation in response to a variety of stimuli (Fig. 2) but displayed normal stress-induced apoptosis as the same level as wild-type cells (Fig. 3). Another stress-responsive MAPK, p38, was not involved in the stress-induced apoptosis (Fig. 4). Second, Bax was capable of translocating into mitochondrial membranes in response to UV irradiation in *sek1*$^{-/-}$ *mkk7*$^{-/-}$ ES cells as observed in the wild-type cells (Fig. 5). Third, the apoptosis in response to various stresses such as UV, etoposide, tunicamycin, and anisomycin occurred even in *sek1*$^{-/-}$ *mkk7*$^{-/-}$ MEF-like cells. Therefore, there must be a SAPK/JNK-independent signaling that is required for the initiation of stress-induced apoptosis in ES and MEF-like cells.

To examine the involvement of MKK7 in cell cycle and senescence, we have recently prepared *mkk7*$^{-/-}$ MEFs from mouse embryos. Interestingly, early passaged wild-type and *mkk7*$^{-/-}$ MEFs showed comparable extent and kinetics of cell death in response to UV irradiation; however, at late time points of culture (after getting cellular immortality), *mkk7*$^{-/-}$ MEFs displayed a resistance to the UV-induced apoptosis.[2] These results suggested that the resistance to UV response observed in *Jnk1*$^{-/-}$ *Jnk2*$^{-/-}$ and *mkk4*$^{-/-}$ *mkk7*$^{-/-}$ MEFs (16, 17) might have some relations to cellular immortality. Because SAPK/JNK activation is crucial for hepatoblast proliferation (12), the immortalized MEFs may lose the regulation of checkpoint in cell cycle and result in resistance to stress-induced apoptosis due to impaired G_1 growth arrest. Therefore, it will be interesting to find out whether re-expression of JNK1 plus JNK2 in *Jnk1*$^{-/-}$ *Jnk2*$^{-/-}$ or MKK4 plus MKK7 in *mkk4*$^{-/-}$ *mkk7*$^{-/-}$ MEFs can restore the apoptotic response to UV stress.

However, recent reports with *Jnk1*$^{-/-}$ *Jnk2*$^{-/-}$ mice clearly show that SAPK/JNK activation is required not only for anti-apoptosis but also for pro-apoptosis in the development of mouse fetal brain (14, 15). There was a reduction of cell death in the lateral edges of hind brain prior to neural tube closure. In contrast, there was increased apoptosis and caspase activation in the forebrain in *Jnk1*$^{-/-}$ *Jnk2*$^{-/-}$ mouse embryos. Thus, SAPK/JNK activation plays a pro-apoptotic role under some circumstances. SAPK/JNK activation may be involved in regulating apoptosis indirectly rather than directly.

SAPK/JNK is activated in T cells by co-stimulation with antigen and CD28 receptors and regulates the production of growth factor IL-2 and cell proliferation (29). Previously, we reported impaired CD28-mediated IL-2 production and proliferation in *sek1*$^{-/-}$ T lymphocytes (23). It has recently been reported that activation of wild-type CD8$^+$ T cells in the presence of different concentrations of SP600125 caused a dose-dependent inhibition of IL-2 production and cell proliferation (30). Thus, SAPK/JNK activation plays an important role in T cell functions. IL-1 is a pro-inflammatory cytokine in inflamed tissues, and the molecular mechanism of IL-1-induced gene expression will yield novel molecular targets for anti-inflammatory therapy. It has been reported that SAPK/JNK activation is required for the gene expression of a cytokine IL-6 and a chemokine IL-8 in a human epidermal carcinoma cell line by using overexpression of a catalytically inactive mutant or antisense RNA of SAPKβ (31, 32). These results indicate that IL-1-mediated activation of SAPK/JNK induces the phosphorylation of a Jun family of component(s) of activator protein-1, resulting in the gene expression of IL-6 and IL-8. In this study, we have also observed the impaired IL-1-mediated IL-6 gene expression both in *sek1*$^{-/-}$ *mkk7*$^{-/-}$ MEF-like cells and in SP600125-treated wild-type cells (Fig. 7). These results provide the first genetic link between SAPK/JNK activation and IL-6 gene expression using gene-disrupted cells and also indicate that SAPK/JNK activation provides a crucial and specific signal for immune responses. Thus, the molecular switch, SAPK/JNK activation, regulates cell proliferation and gene expres-

[2] T. Wada, N. Joza, H.-Y. M. Cheng, T. Sasaki, I. Kozieradzki, M. Nghiem, K. Bachmaier, T. Katada, H. Nishina, and J. M. Penninger, submitted for publication.

sion in embryonic development and immune responses rather than stress-induced apoptosis.

Acknowledgments—We thank Dr. Izumu Saito and RIKEN BRC for providing us with adenovirus-encoding Cre recombinase. We also thank Dr. James R. Woodgett for suggestions and criticism.

REFERENCES

1. Peng, L., Deepak, N., Imawati, B., Srinivasa, M. S., Manzoor A., Emad, S. A., and Xiaodong, W. (1997) *Cell* **91,** 479–489
2. Orrenius, S., Zhivotovsky, B., and Nicotera, P. (2003) *Nature Rev. Mol. Cell Biol.* **4,** 552–565
3. Yoshida, H., Kong, Y.-Y., Yoshida, R., Elia, A. J., Hakem, A., Hakem, R., Penninger, J. M., and Mak, T. W. (1998) *Cell* **94,** 739–750
4. Davis, R., J. (2000) *Cell* **103,** 239–252
5. Chang, L., and Karin M. (2001) *Nature* **410,** 37–40
6. Manning, A. M., and Davis, R. J. (2003) *Nature Rev. Mol. Drug Disc.* **2,** 554–565
7. Lawler, S., Fleming, Y., Goedert, M., and Cohen, P. (1998) *Curr. Biol.* **8,** 1387–1390
8. Wada, T., Nakagawa, K., Watanabe, T., Nishitai, G., Seo, J., Kishimoto, H., Kitagawa, D., Sasaki, T., Penninger, J. M., Nishina, H., and Katada, T. (2001) *J. Biol. Chem.* **276,** 30892–30897
9. Kishimoto, H., Nakagawa, K., Watanabe, T., Kitagawa, D., Momose, H., Seo, J., Nishitai, G., Shimizu, N., Ohata, S., Tanemura, S., Asaka, S., Goto, T., Fukushi, H., Yoshida, H., Suzuki, A., Sasaki, T., Wada, T., Penninger, J. M., Nishina, H., and Katada, T. (2003) *J. Biol. Chem.* **278,** 16595–16601
10. Ganiatsas, S., Kwee, L., Fujiwara, Y., Perkins, A., Ikeda, T., Labow, M. A., and Zon, L. I. (1998) *Proc. Natl. Acad. Sci. U. S. A.* **95,** 6881–6886
11. Nishina, H., Vaz, C., Billia, P., Nghiem, M., Sasaki, T., Pompa, J. L., Furlonger, K., Paige, C., Hui, C.-C., Fischer, K. D., Kishimoto, H., Iwatsubo, T., Katada, T., Woodgett, J. R., and Penninger, J. M. (1999) *Development* **126,** 505–516
12. Watanabe, T., Nakagawa, K., Ohata, S., Kitagawa, D., Nishitai, G., Seo, J., Tanemura, S., Shimizu, N., Kishimoto, H., Wada, T., Aoki, J., Arai, H., Iwatsubo, T., Mochita, M., Watanabe, T., Satake, M., Ito, Y., Matsuyama, T., Mak, T. W., Penninger, J. M., Nishina, H., and Katada, T. (2002) *Dev. Biol.* **250,** 332–347
13. Lin, A. (2002) *BioEssays* **25,** 17–24
14. Kuan, C.-Y., Yang, D. D., Roy, D. R. S., Davis, R. J., Rakic, P., and Flavell, R. A. (1999) *Neuron* **22,** 667–676
15. Sabapathy, K., Jochum, W., Hochedlinger, K., Chang, L., Karin, M., and Wagner, E. F. (1999) *Mech. Dev.* **89,** 115–124
16. Tournier, C., Hess, P., Yang, D. D., Xu, J., Turner, T. K., Nimnual, A., Bar-Sagi, D., Jones, S. N., Flavell, R. A., and Davis, R. J. (2000) *Science* **288,** 870–874
17. Tournier, C., Dong, C., Turner, T. K., Jones, S. N., Flavell, R. A., and Davis, R. J. (2001) *Genes Dev.* **15,** 1419–1426
18. Aoki, H., Kang, P. M., Hampe, J., Yoshimura, K., Noma, T., Matsuzaki, M., and Izumo, S. (2002) *J. Biol. Chem.* **277,** 10244–10250
19. Chauhan, D., Li, G., Hideshima, T., Podar, K., Mitsiades, C., Mitsiades, N., Munshi, N., Kharbanda, S., and Anderson, K. C. (2003) *J. Biol. Chem.* **278,** 17593–17596
20. Nishina, H., Fischer, K. D., Radvanyi, L., Shahinian, A., Hakem, R., Rubie, E. A., Bernstein, A., Mak, T. W., Woodgett, J. R., and Penninger, J. M. (1997) *Nature* **385,** 350–353
21. Kanegae, Y., Lee, G., Sato, Y., Tanaka, M., Nakai, M., Sasaki, T., Sugano, S., and Saito, I. (1995) *Nucleic Acids Res.* **23,** 3816–3821
22. Kitagawa, D., Tanemura, S., Ohata, S., Shimizu, N., Seo, J., Nishitai, G., Watanabe, T., Nakagawa, K., Kishimoto, H., Wada, T., Tezuka, T., Yamamoto, T., Nishina, H., and Katada, T. (2002) *J. Biol. Chem.* **277,** 366–371
23. Nishina, H., Bachmann, M., Oliveira-dos-Santos, A. J., Kozieradzki, I., Fischer, K. D., Odermatt, B., Wakeham, A., Shahinian, A., Takimoto, H., Bernstein, A., Mak, T. W., Woodgett, J. R., Ohashi, P. S., and Penninger, J. M. (1997) *J. Exp. Med.* **186,** 941–953
24. Beere, H. M., Wolf, B. B., Cain, K., Masser, D. D., Mahboubi, A., Kuwana, T., Tailor, P., Morimoto, R. I., Cohen, G. M., and Green, D. R. (2000) *Nat. Cell Biol.* **2,** 469–475
25. Saleh, A., Srinivasula, S. M., Balkir, L., Robbins, P. D., and Alnemri, E. S. (2000) *Nat. Cell Biol.* **2,** 476–483
26. Bruey, J.-M., Ducasse, C., Bonniaud, P., Ravagnant, L., Susin, S. A., Diaz-Latoud, C., Gurbuxani, S., Arrigo, A.-P., Kroemer, G., Solary, E., and Garrido, C. (2000) *Nat. Cell Biol.* **2,** 645–652
27. Xia, Z. G., Dickens, M., Raingeaud, J., Davis, R. J., and Greenberg, M. E. (1995) *Science* **270,** 1326–1331
28. Putcha, G. V., Le, S., Frank, S., Besirli, C. G., Clark, K., Chu, B., Alix, S., Youle, R. J., LaMarche, A., Maroney, A. C., and Johnson, E. M., Jr. (2003) *Neuron* **38,** 899–914
29. Su, B., Jacinto, E., Hibi, M., Kallunki, T., Karin, M., and Ben-Neriah, Y. (1994) *Cell* **77,** 727–736
30. Conze, D., Krahl, T., Kennedy, N., Weiss, L., Lumsden, J., Hess, P., Flavell, R. A., Gros, G. L., Davis, R. J., and Rincon M. (2002) *J. Exp. Med.* **195,** 811–823
31. Krause, A., Holtmann, H., Eickemeier, S., Winzen, R., Szamel, M., Resch, K., Saklatvala, J., and Kracht, M. (1998) *J. Biol. Chem.* **273,** 23681–23689
32. Holtmann, H., Enninga, J., Kalble, S., Thiefes, A., Dorrie, A., Broemer, M., Winzen, R., Wilhelm, A., Ninomiya-Tsuji, J., Matsumoto, K., Resch, K., and Kracht, M. (2001) *J. Biol. Chem.* **276,** 3508–3516

ELSEVIER

Mechanisms of Development 121 (2004) 791–802

www.elsevier.com/locate/modo

Research paper

Mutations affecting liver development and function in Medaka, *Oryzias latipes*, screened by multiple criteria

Tomomi Watanabe[a], Satoshi Asaka[a], Daiju Kitagawa[a], Kota Saito[a], Ryumei Kurashige[a], Takao Sasado[b], Chikako Morinaga[b], Hiroshi Suwa[b], Katsutoshi Niwa[b], Thorsten Henrich[b], Yukihiro Hirose[c], Akihito Yasuoka[d], Hiroki Yoda[e], Tomonori Deguchi[e], Norimasa Iwanami[f], Sanae Kunimatsu[f], Masakazu Osakada[e], Felix Loosli[h], Rebecca Quiring[h], Matthias Carl[h], Clemens Grabher[h], Sylke Winkler[h], Filippo Del Bene[h], Joachim Wittbrodt[h], Keiko Abe[d], Yousuke Takahama[f], Katsuhito Takahashi[g], Toshiaki Katada[a], Hiroshi Nishina[a,*], Hisato Kondoh[b], Makoto Furutani-Seiki[b,*]

[a]*Department of Physiological Chemistry, Graduate School of Pharmaceutical Sciences, University of Tokyo, Tokyo 113-0033, Japan*
[b]*ERATO, Jaman Science and Technology Corporation, Kondoh Differentiation Signaling Project, Kawara-cho 14, Yoshida, Sakyo-ku, Kyoto 606-8305, Japan*
[c]*Graduate School of Biostudies, Kyoto University, Kyoto 606-8501, Japan*
[d]*Department of Applied Biological Chemistry, University of Tokyo, Tokyo 113-0033, Japan*
[e]*Graduate School of Frontier Biosciences, Osaka University, Osaka 565-0871, Japan*
[f]*Division of Experimental Immunology, Institute for Genome Research, The University of Tokushima, Tokushima 770-8503, Japan*
[g]*Department of Molecular Medicine and Pathophysiology, Research Institute, Osaka Medical Center for Cancer and Cardiovascular Diseases, Osaka 537-8511, Japan*
[h]*Developmental Biology Programme, EMBL Heidelberg, Meyerhofstrasse 1, D-69117, Heidelberg, Germany*

Received 20 January 2004; received in revised form 30 March 2004; accepted 3 April 2004

Abstract

We report here mutations affecting various aspects of liver development and function identified by multiple assays in a systematic mutagenesis screen in Medaka. The 22 identified recessive mutations assigned to 19 complementation groups fell into five phenotypic groups. Group 1, showing defective liver morphogenesis, comprises mutations in four genes, which may be involved in the regulation of growth or patterning of the gut endoderm. Group 2 comprises mutations in three genes that affect the laterality of the liver; in *kendama* mutants of this group, the laterality of the heart and liver is uncoupled and randomized. Group 3 includes mutations in three genes altering bile color, indicative of defects in hemoglobin–bilirubin metabolism and *globin* synthesis. Group 4 consists of mutations in three genes, characterized by a decrease in the accumulation of fluorescent metabolite of a phospholipase A_2 substrate, PED6, in the gall bladder. Lipid metabolism or the transport of lipid metabolites may be affected by these mutations. Mutations in Groups 3 and 4 may provide animal models for relevant human diseases. Group 5 mutations in six genes affect the formation of endoderm, endodermal rods and hepatic bud from which the liver develops. These Medaka mutations, identified by morphological and metabolite marker screens, should provide clues to understanding molecular mechanisms underlying formation of a functional liver.

Keywords: Liver development; Medaka; Hepatoblast; Hepatic bud; Laterality; Gall bladder; Lipid metabolism; Endoderm formation; Bile; Zebrafish

1. Introduction

The liver is an organ with vital functions, including processing and storage of nutrients, maintenance of serum composition, detoxification and bile production. The major functional cells of a liver are the hepatocytes

* Corresponding authors. Tel.: +81-75-771-9362; fax: +81-75-771-3835 (M. Furutani-Seiki); Tel.: +81-3-5841-4754; fax: +81-3-5841-4751 (H. Nishina).
E-mail addresses: furutani@dsp.jst.go.jp (M. Furutani-Seiki), nishina@mol.f.u-tokyo.ac.jp (H. Nishina).

0925-4773/$ - see front matter © 2004 Elsevier Ireland Ltd. All rights reserved.
doi:10.1016/j.mod.2004.04.004

and cholangiocytes (bile duct cells). The common progenitors of hepatocytes and cholangiocytes are derived from hepatoblasts in the hepatic endoderm. The hepatic endoderm arises from the foregut endoderm that interacts with adjacent tissues, such as the cardiac mesoderm and septum transversum mesenchyme (Douarin, 1975; Grapin-Botton and Melton, 2000; Tam et al., 2003; Zaret, 2001). The vasculature is another important component of the liver. Angioblasts, which are endothelial cell precursors, accumulate around the liver bud and become interspersed with the hepatoblasts (Matsumoto et al., 2001).

Regulatory genes that are crucial for liver formation have been isolated in mice and confirmed by reverse genetics (see Zaret, 2002 for a review). For instance, we have shown using SEK1 or MKK7-deficient mice that two stress-signaling kinases, SEK1 (also called MKK4) and MKK7, play crucial roles in hepatoblast proliferation and survival (Nishina et al., 1999; Wada et al., 2004; Watanabe et al., 2002). Although a reverse genetic approach is powerful in characterizing functions of known genes, knowledge of genes, particularly in hepatic bud formation from endoderm, morphogenesis and laterality of the liver, and hemoglobin–bilirubin or lipid metabolism, is still limited. Therefore, identifying mutations affecting these aspects of liver formation and function will uncover genes required for these processes.

Systematic forward genetic screens for mutations affecting embryogenesis have been carried out in zebrafish. Zebrafish embryos are transparent and sustain defects in circulation or hematopoiesis, because oxygen supplied by simple diffusion is sufficient for development and the liver is not the site of embryonic hematopoiesis (Alexander and Stainier, 1999). These characteristics of zebrafish have enabled the study of genes involved in the development of endoderm, cardiovascular and hematopoietic systems. Zebrafish mutants with impaired endoderm formation, degenerative liver, impaired lipid metabolism in the intestine and hepatobiliary system, have been identified (Chen et al., 1996; Farber et al., 2001; Pack et al., 1996; Schier et al., 1996, 1997; Zhang et al., 1998). Furthermore, the availability of transgenic lines expressing GFP throughout the digestive system allows direct observation of the endoderm and digestive organ formation in living embryos (Field et al., 2003; Ober et al., 2003). However, genes identifiable in a single model organism by the mutational approach are limited due to a functional overlap of genes in vertebrates.

Medaka is evolutionally distant from zebrafish and interspecies differences in the functional overlap of genes allow identification of mutations as yet unidentified in zebrafish. The liver and gall bladder are more conspicuous in living embryos in Medaka than in zebrafish. Medaka has a smaller genome size (half that of zebrafish, and only double that of Fugu), inbred strains are available, and a wide range of growth temperatures facilitates identification of temperature sensitive mutations.

Taking advantage of these attributes of Medaka, we have carried out a mutagenesis screen, using multiple assays to detect defects in various aspects of the development of a functional liver. These include not only morphological assays, but also those of the functions related to the liver, such as hemoglobin–bile and lipid metabolism. In this report, we present the initial characterization of mutations isolated in the screen, ranging from those affecting endoderm formation to those affecting liver physiology in Medaka.

2. Results

2.1. Designing of mutant screening based on multiple criteria

2.1.1. Morphological screening

We carried out the morphological screen of the liver by inspecting live embryos when the liver became discernible from 4 days post-fertilization (dpf, stage (st.) 32) at 28 °C and the gall bladder became prominent at approximately 120 h post-fertilization (hpf, st. 36). The lateral views of wild-type embryos and livers at st. 32 and 36 are shown in Fig. 1A–C. The liver, gall bladder, and blood vessel from the liver connected to the Cuvierian duct developing on the left side of the embryo were observed (Fig. 1B,C).

To analyze the time course of liver development, we carried out in situ hybridization between st. 21 and 39 using endoderm-specific markers, *foxA3* and *gata6* (Fig. 1D–P). The hepatic bud formed from the endoderm rod in wild-type Medaka at st. 25 (Fig. 1H,I). At st. 27 the liver began to enlarge and the swim bladder appeared from the gut tube and began to enlarge (Fig. 1J–P, arrowheads and asterisks indicate the liver and swim bladder, respectively). *foxA3* was also expressed in the pharynx, but unlike in zebrafish, *foxA3* was not expressed in the pancreas in Medaka (data not shown). On the other hand, the expression of *gata6* was restricted to the liver from st. 25 to 31 (Fig. 1I,K,M). Soon after at st. 31, we screened live embryos. No expression of *gata6* was detected in the liver at st. 34 (Fig. 1O). In zebrafish, *gata6* is expressed in the liver and gut. Thus, the expression pattern of *gata6* in Medaka is different from that in zebrafish.

Considering the relatively late development of the liver in embryogenesis, care was taken to avoid isolating mutants showing a general retardation of development. Mutants with altered liver morphologies, such as the size, shape, and laterality of livers, were screened first at st. 32 and confirmed at st. 36 when the liver and gall bladder became larger in wild-type embryos.

2.1.2. Screening of gall bladder color

Based on the assumption that impaired bile metabolism in the liver results in an abnormal color of bile, we inspected

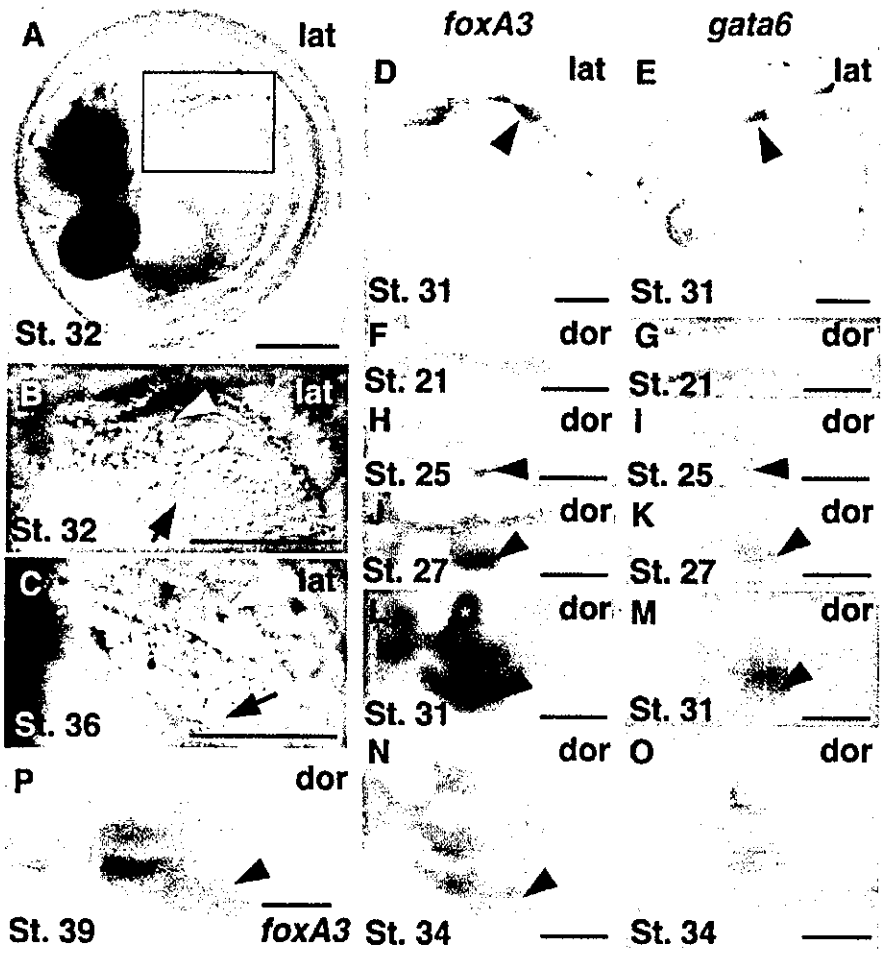

Fig. 1. Liver development in Medaka. Live (A–C) and fixed wild-type embryos stained by in situ hybridization using the *foxA3* (D, F, H, J, L, N, and P) and *gata6* (E, G, I, K, M, and O) probes. (A–C, D, and E) Lateral view; (F–P) Dorsal view. (A–C) The liver was readily visible from the left side of living embryos at st. 32 (A and B) and st. 36 (C) when screening was carried out; (F and G) st. 21; (H and I) The hepatic bud was formed at st. 25 and subsequently liver growth occurred; (J and K) st. 27; (L and M) st. 31; (N and O) st. 34 and (P) st. 39. White broken line demarcates the liver. White arrowheads and black arrows indicate the gall bladder and the vein of the liver, respectively. Black arrowheads and white asterisks show the hepatic bud and the liver, and the swim bladders, respectively. lat: lateral, dor: dorsal. Scale bars correspond to 200 μm.

color of bile in the gall bladder. Bile in the wild-type embryo at st. 35 was light green. Impaired erythropoiesis was reported to alter bile color in zebrafish (Shafizadeh et al., 2002). To distinguish mutations affecting erythropoiesis from those affecting bile metabolism in the liver, we carried out hemoglobin staining with *o*-dianisidine and in situ hybridization analysis using embryonic globins such as *α-0*, *α-1*, and *β-1 globins*.

2.1.3. Screening using fluorescent phospholipid reporters

We used a fluorescent phospholipid reporter, PED6, to screen for mutations affecting lipid metabolism (Farber et al., 2001).

PED6 is a synthetic substrate for PLA_2 that becomes fluorescent after cleavage in the intestine and its fluorescent PED6 metabolites undergo rapid hepatobiliary transport, labeling the liver before the gall bladder, as shown in Fig. 5C. Embryos administered with PED6 showed intense fluorescence in the gall bladder, liver and intestinal lumen. We screened for embryos showing an impaired accumulation of the fluorescent metabolites of PED6. To exclude mutations affecting the swallowing of PED6, the unquenched form of PED6, BODIPY-FL-C5, was used.

2.1.4. Rescreening for mutations affecting early embryogenesis using the foxA3 probe

In addition to directly screening for liver associated phenotypes, we also screened for mutations affecting endoderm and hepatic bud formations among mutants that were initially identified on the basis of morphological abnormalities (Furutani-Seiki et al., 2004). To this end, we carried out in situ hybridization using *foxA3* at st. 28 (Fig. 1J).

2.2. Mutations affecting formation and function of the liver isolated by the multi-assay screen

By screening 210 F2 families, we have isolated 19 mutations. Since all of the mutations were zygotic recessive mutations, mutants refer to homozygotes of these mutations in this report. These mutations were classified into the following five phenotypic groups and features of these mutations were summarized in Table 1.

2.2.1. Mutations affecting liver morphogenesis

Mutations in four genes, *kakurembo* (*kak*), *hiohgi* (*hio*), *origami* (*ora*) and *kamifusen* (*kam*) affect liver morphology.

In live *kak* embryos at st. 34, the liver was not clearly discernible at the position where it should be formed and the gall bladder was dislocated anteriorly (Fig. 2A,B). In *kak* mutant embryos at st. 24, the expression level of *gata6* in the liver markedly reduced, while that of *cardiac myosin light chain* (*mlc*) in the heart was unaltered (Fig. 2G,H). In *kak* mutant embryos at st. 34, the expression level of *foxA3* was also greatly reduced (Fig. 2I,J). Since liver budding appeared to occur in *kak* mutants, *kak* may be required for the growth or maintenance of the liver. The gut tube was undulated at st. 36 (data not shown) without affecting the epithelial structure of the gut tube (Fig. 2N,O,Q,R).

In *hio* mutant embryos at st. 36 and at later stages, the liver was small and malformed (Fig. 2C,D, and data not shown). In situ hybridization using the *gata6* probe clearly showed impaired liver formation in *hio* mutant embryos at st. 30 (Fig. 2K,L). In addition to the liver defects, *hio* mutant embryos also lacked pectoral fins and died after hatching.

In *kam* mutant embryos, blood accumulated in the liver, and the liver was malformed (Fig. 2E). The expression of *gata6* appeared normal (Fig. 2M).

In *ora* mutant embryos at st. 36, the liver shape was altered, the gall bladder was displaced and the gut undulated (Fig. 2F). *ora* mutant embryos at st. 40 have an enlarged swim bladder and undulated gut, whereas the heart and kidneys appeared unaltered (Fig. 2T,U). Cross sections at the level of the liver, gut tube, and yolk showed that hepatocytes seemed normal, but the embryo itself lay apart from the yolk and the intestine was malformed (Fig. 2P,S). In contrast to regularly aligned polarized epithelial cells in

Table 1
Mutations affecting liver formation and function

Genes	Alleles	Viability	Phenotypes	Other phenotypes	References
Group 1: Mutations affecting liver morphogenesis					
kakurembo (kak)	*j140-3B*	Embryonic lethal	Small and mislocated liver	Mislocated gall bladder, undulated gut	
hiohgi (hio)	*j102-5B*	Embryonic viabe	Small liver	Fin missing	
kamifusen (kam)	*j124-4A*	Embryonic lethal	Malformed liver	Blood accumulated near the liver	
origami (ora)	*j137-1A*	Embryonic viable	Malformed liver	Undulated gut, enlarged swim bladder	
Group 2: Mutations affecting liver laterality					
kendama (ken)	*j103-11C*	Develop to adult fish	Inverted positions of liver and gall bladder	Medially located liver and missing spleen	
hanetsuki (hat)	*j68-7A*	Develop to adult fish	Inverted positions of liver and gall bladder	Inverted heart looping	
dendendaiko (den)	*j73-11A*	Develop to adult fish	Inverted positions of liver and gall bladder	Inverted heart looping	
Group 3: Mutations affecting bile color in the gall bladder					
akane (aka)	*j140-8A*	Embryonic lethal	Deep red bile	Colorless erythrocytes	
suou (suo)	*j98-5A*	Adult viable	Light red bile	Erythrocytes were faint red	
ominaeshi (omi)	*j24-13E*	Embryonic lethal	Colorless bile	Colorless erythrocytes	
Group 4: Mutations affecting lipid metabolism					
ukon (uko)	*j152-8A*	Embryonic lethal	Failure in metabolizing PED6	Edematic after hatching	a
aonibi (aon)	*j60-3A/j9-2F*	Embryonic lethal	Failure in metabolizing PED6	Small and degenerated forebrain at st. 38	
uguisucha (ugu)	*j153-9A*	Embryonic lethal	Failure in metabolizing PED6	Growth retardation after hatching	
Group 5: Mutations affecting endoderm formation					
akatsuki (aku)	*j22-15A/jf121-1A*	Embryonic lethal	Lacking *foxA3* expression	Similar to the zebrafish *oep* phenotype	a,b
akebono (ake)	*j54-7A*	Embryonic lethal	Lacking *foxA3* expression	Similar to the zebrafish *oep* phenotype	a,b
mochizuki (moc)	*j96-11B*	Embryonic lethal	Lacking *foxA3* expression	Similar to the zebrafish *oep* phenotype	a,b
sakura (sak)	*jr10-4A/j153-3A*	Embryonic lethal	Lacking the hepatic bud	Loss of heart and degeneration of eyes	b
hirame (hir)	*j54-20C*	Embryonic lethal	Defect in hypoblast convergence	Flat embryo	a,b
fukuwarai (fku)	*j8-33A/j93-4A*	Embryonic lethal	Lacking the hepatic bud	Cell polarity and alignment affected	a,b

References: a, Kitagawa et al., 2004; b, Furutani-Seiki et al., 2004.